STUDY OF STRUCTURAL AND ELECTRONIC PROPERTIES OF ANTIMONY AND BISMUTH

A Dissertation

Submitted for the Partial Fulfillment of

Requirements for the Masters of Science Degree in Physics

Surya Prasad Ghimire

T.U. Registration No: 5-1-19-142-2004

Symbol No: Phy. 1319/072

DEPARTMENT OF PHYSICS

INSTITUTE OF SCIENCE AND TECHNOLOGY

BIRENDRA MULTIPLE CAMPUS,

BHARATPUR CHITWAN

October, 2020

DECLARATION

I, "Surya Prasad Ghimire", hereby declare that the work presented here is genuine work done originally by me and has not been published or submitted elsewhere for the requirement of a degree program. Any literature, data or works done by others and cited in this dissertation has been given due acknowledgement and listed in the reference.

_____

Surya Prasad Ghimire

Date:

RECOMMENDATION LETTER

This is to certify that the dissertation work entitled **STUDY OF STRUCTURAL AND ELECTRONIC PROPERTIES OF ANTIMONY AND BISMUTH** has been carried out by "**Surya Prasad Ghimire"** as the partial fulfillment for the requirement of M.Sc. Degree in Physics under my supervision. To the best of my knowledge, this work is original and is not been submitted to any other degree in this institute.

…….

Supervisor
Prof. Dr. Sitaram Bahadur Thapa
Department of Physics
Birendra Multiple Campus
Tribhuvan University
Bharatpur, Nepal
Date…….

…….

Supervisor
Dr. Rajendra Prasad Adhikari
Department of Natural Science
(Applied Physics)
Kathmandu University
Dhulikhel, Kavre
Date…….

ABSTRACT

We optimize lattice parameter and identify the nature and values of band gap of Antimony and Bismuth by using quantum espresso.This work includes the general introduction on crystal structure and different models that work in the lattice constant and lattice dynamic. We also briefly include various theoretical details such as Born-Oppenheimer Approximation, Hartree-Fock Approximation, Density Functional Theory, Kohn-Sham approach, Local Density approximation, Generalized Gradient Approximation, and pseudo- potential. Finally, we discussed the fundamentals of Quantum Espresso computational program with the result and discussion on electronic properties, kinetic energy cut-off, lattice parameter, band gap, density of state and partial density of state of Antimony and Bismuth.

We optimize lattice parameter and identify the nature and values of band gap of Antimony and Bismuth structure. Optimized value of the lattice parameter, kinetic energy (cut off energy),K-point grid and band gap of Antimony is obtained as 8.2870 au ,80 Ry,8×8×8 and 0.15eV respectively. Similarly,Optimized value of the lattice parameter, kinetic energy (cut off energy),K-point grid and band gap of Bismuth is obtained as 4.7459001541 Bohr ,65 Ry,10×10×10 and 0.09eV respectively.We used norm-conserving pseudo potentials; self consistent calculations employed Density Functional Theory (DFT) under Generalized Gradient Approximation (GGA) by using Quantum ESPRESSO package.

ACKNOWLEDGEMENT

In this insightful delight I would first of all convey my sincere gratefulness and express my humble gratitude to my respected supervisors Prof. Dr. Sitaram Bahadur Thapa for introducing me semimetals elements of group 15 .I moreover would like to specific my appreciation his patience, fruitful counselling, support, commitment and regular motivation.

I would also like to express my deepest gratitude to our supervisor Dr. Rajendra Prasad Adhikari. His efficient computational concept, practical advices, enduring encouragement as well as valuable time helps for correction and complete my task.

Moreover, my gratitude also goes to former Campus Chief Mr. Govinda Sapkota and present Campus Chief Prof. Dayaram Poudel (Birendra Multiple Campus) and Prof. Arun Kumar Shrestha (Head of Department of Physics, Birendra Multiple Campus) for their warm afflatus and encouragement. I am very thankful to Dr. Seshkant Adhikari, Prof. Dr. Harihar Poudyal, Associate Prof. Dilli Prasad Sapkota, Mr. Ekraj Poudel, Mr. Rajendra Neupane, Mr. Moti Bhusal, Mr. Udaya Bahadur Thapa, Mr. Ramkrishna Tiwari, Mr. Rabindra Raj Bista, Mr. Madan Phuyal, Mr. Ishwor Chandra Poudel , Mr. Sanjaya Shah, Mr. Pratap Koirala, and all respective Physics Department Members of Birendra Multiple campus.

My appreciation also goes to energetic and supportive colleagues Mr. Rajesh Poudel, Mr. Surya Prasad Ghimire, Mr. Amrit Sharma, Mr. Shiva Prasad Bhusal, Mr. Bishnu Dhakal, Mr. Diwakar Devkota and all classmates for the stimulating discussion, advice and all the memorable moments. Also, I would like to give special thanks to Mr. Bishnu Karkee for kind support and suggestion. Also, my remembrance goes to my family members for their treasured sustainment and encouragement during my academic years. My huge respect goes to my father Mr. Chandra Bilas Ghimire, mother Bishnumaya Ghimire, wife Sunita Dhakal, daughter Suyogya Ghimire, sisters and all relatives who continuously showed their pinnacle efforts for the succession of this paper.

.....……...

Surya Prasad Ghimire
Birendra Multiple Campus
Bharatpur Chitwan
2020

TABLE OF CONTENTS

LIST OF TABLES

LIST OF FIGURES

LIST OF ABBREVIATIONS

BO	:	Born Oppenheimer
CP	:	Car-Perrinello
CPMD	:	Car-Parrinello Molecular Dynamics
DFPT	:	Density Functional Perturbation Theory
DFT	:	Density Functional Theory
DOS	:	Density of State
FPMD	:	First Principle Molecular Dynamics
GGA	:	Generalized Gradient Approximation
HEG	:	Homogeneous Electron Gas
HF	:	Hartree-Fock
HK	:	Hohenberg-Kohn
KS	:	Kohn-Sham
LDA	:	Local Density Approximation
MBE	:	Molecular Beam Epitaxy
MOVPE	:	Metalorganic Vapour Phase Epitaxy
NSCF	:	Non-Self Consistent Field
PBE	:	Perdew, Burke and Ernzerhof
PDOS	:	Partial Density of State
PP	:	Pseudo Potential
PW	:	Plane Wave
QE	:	Quantum ESPRESSO
SCF	:	Self Consistent Field
XC	:	exchange Correlation

CHAPTER 1

INTRODUCTION

1.1 General Consideration

The ancient physicist started their study on the physics from the matter. Matter can be defined as anything which has mass and occupies a volume. After long study on the matter and its constituents, physicists and chemists have found that all the matter in nature have made up of indivisible unit which is called atom. Latter came to be known that matter mean atom and other particle which has mass and occupies volume. So, all the matter which constitutes our environment are made up of atoms or molecules. Inside the matter these atoms or molecules are held together by some interacting forces. Depending upon these interacting forces, the different matters have different properties. One of the main properties of the matter arisen due to such interaction is the state of matter. That means depending upon the interaction between the atoms or molecules in matter, there are generally three states of matter i.e gaseous, liquid and solid state.

In solid state the particles mean constituents that may be atoms, ions or molecules and are densely packed with intense interaction forces to give a definite shape and volume. The interaction force is so strong that the particles can't move freely but can only vibrate about their equilibrium position. These strong interaction forces are responsible for the different properties like mechanical, thermal, electrical, magnetic and optical properties of the solid. These properties of solid deals by a branch of physics called solid state physics. The constituent of the solid that is atoms, ions or molecules in solid are arranged in an orderly repeating pattern i. e. regular pattern.The formation of crystalline or amorphous solid depends upon the material involved and the solidification or freezing of matter may lead to formation of ordered or disordered state in which ordered state is known as crystalline state where as the disordered one is termed the amorphous state. [1]

Crystalline state refers to an infinitive array of atoms or a group of atoms. The whole volume of crystal is constructed by moving block of smallest size along its edges which block is called a unit cell. The three-dimensional structure of a crystal is built from a repetitive arrangement of the simplest structural unit, called the unit cell, just as a single tile is often a unit cell for a two-dimensional ceramic tiling pattern. It received direct experimental configuration in 1913 through the work of W. and L. Bragg, who founded the subject of X-ray crystallography and began investigation of ow atoms arranged in solids. Depending on the nature of the unit cell, Bragg's law is satisfied only at certain orientations of the crystal, and a beam of X-rays will then emerge from the crystal at a certain angle to the incident beam. Bragg's law requires that the diffracted radiation from different layers of unit cells be in phase.To show visualization of motional operations performed on atoms with unit cell every crystal structure satisfies the requirements of a specific group of certain *symmetry operation* accordingly.[2]

Crystals

Crystals may be classified in terms of the dominant type of chemical binding force keeping the atoms together. All these bonds involve electrostatic forces, with the chief differences among them lying in the ways in which the outer electrons of the structural elements are distributed. The distinct types of bonds that provide the cohesive forces in crystals can be classified as follows: (i) the ionic bond (ii) the covalent bond (iii) the metallic bond (iv) the van der Waals bond and (v) the hydrogen bond.

i)The ionic bond

The electron state is little affected by the coming together of the ions to from the solid and the interaction of any two ions within the solid can be represented by the interionic potential curve of two isolated ions. At large separation the interionic potential is dominated by the long-range

electrostatic interaction $\frac{\pm e^2}{4\pi\varepsilon_0 r;}$ the +sign for two ions of same sign and -sign for ions of opposite sign [3].

ii)The covalent bond

Covalent bond is the type of chemical bond which is formed due to the sharing of pair of electrons between the combining atoms.The binding energy is associated with the sharing of valence electrons between atoms. The states of the valence electrons are profoundly changed by the approach of the atoms to form the solid, and where an atom forms more than one bond the energy depends strongly on their relative orientation.In an ideal covalent bond between two atoms the two electrons are equally shared.

iii)The metallic bond

Metallic bond constitute the electrostatics attractive forces between the delocalized electrons called conduction electrons gathered in an electron cloud and the positively charged metal ions. Metallic bonds accounts for many physical properties of metals such as strength, malleability, ductility, thermal and electrical conductivity, opacity and luster.

iv)The Vender Wall Bond

A vender wall bond is the weak interaction between the atoms of a substances resulting in soft consistency crystals. The outer orbit of the atom is completely filled with shared electrons but their charge keeps transferring.It is only significant in case where other types of bonding are not possible.For example, between atoms with closed electron shell, or between saturated molecules. The physical source of this bonding is charge fluctuations in the atoms due to zero-point motion.The bonding energy is dependent on the polarizability of the atoms involved and is mostly of order of 0.1eV. Typical atomic bonding radii for van der Waals bonding are

considerably larger than for chemical bonding. Crystal of inert gases like Helium is made by this type of bond.

v)The Hydrogen Bond

Hydrogen bond is formed under certain conditions when a single hydrogen atom appears to be bonded to two distinct electronegative atoms which can be represented as X-H …Y where X is called *donor* while *Y* is called acceptor and *H* is mediator .The bond shown by dotted line is hydrogen bond .Generally,the phenomena related to hydrogen bonding are quite diverse and this sort of bonding is harder to characterize than most other types. The binding energies of hydrogen bonds are of the order of 0.1eV per bond.[1,4]

Lattice symmetry

An infinite array of points in space called a lattice also called space lattice and arrangement of points defined the lattice symmetry. when an atom or a uniform group of atom s attached to each lattice point, we get a crystal structure. The attached atom or group of atoms called basis, which is identical for each lattice point in terms of composition, relative orientation, and separation. The lattice is defined by three fundamental translation vector **a, b** and **c** such the atomic arrangement looks an equivalent in every respect when viewing from the purpose r as when viewed from the purpose . Draw a vector **t** connecting two lattice point P1 and P2 (fig 1.1) represent vectors **r1** and **r2** respectively then, the vector **t** is defined as

$$\vec{r_2} = \vec{r_1} + \vec{t}$$

Such that

$$\vec{t} = n_1\vec{a} + n_2\vec{b} + n_3\vec{c}$$

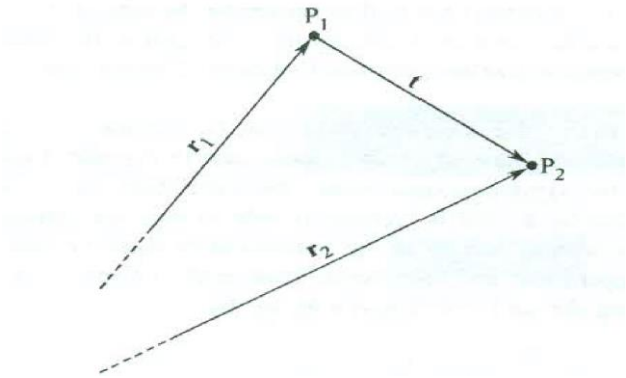

Fig. 1.1: Two lattice points P_1 and P_2 of a three-dimensional lattice connected by translation vector t.

When all the lattice points can be located for the arbitrary choice of only integral values of n_1, n_2 and n_3, the crystal axes **a, b** and **c** are called primitive and the resulting unit is called *primitive cell.* A lattice is a mathematical abstraction; the crystal structure is formed when a basis of atom is attached identically to every lattice point. The logical relation is

Lattice + basis = crystal structure

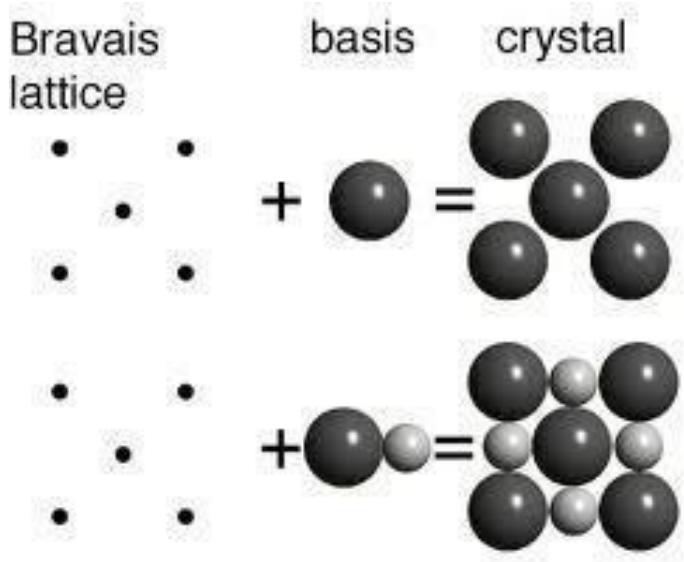

Fig 1.2: crystal structure

An alternate primitive cell is known as Wigner-Seitz cell. A lattice point is joined to all the nearby lattice point s with the help of lattice vectors. Then, a plane perpendicular to each of these vectors, connecting the central lattice point, is draw at the midpoint of the vector. The planes

form a completely closed polyhedron which contains one lattice point at the centre which is named Wigner and Seitz [5].

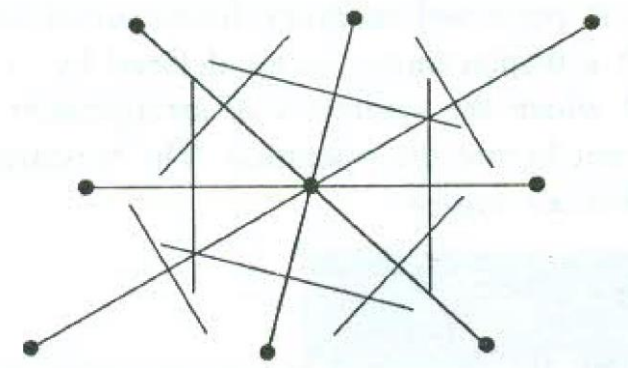

Fig.1.3: The construction of Wigner-Seitz cell for a two-dimensional space lattice.

Lattice planes and miller indices

A well-formed crystal or internal planes through a crystal structure are laid out in terms of Miller Indices, h, k, and l, written in round brackets, (hkl). an equivalent terminology is employed to specify planes during a lattice. Miller indices, (hkl), represent not only one plane, but the set of all identical parallel lattice planes. The values of h, k and l are the reciprocals of the fractions of a unit edge, a, b and c respectively, intersected by an appropriate plane. this suggests that a group of planes that lie parallel to a unit edge is given the index 0 (zero) no matter the lattice geometry. Thus, a group of planes that transit the ends of the unit cells, cutting the a-axis at an edge 1 a, and parallel to the b- and c-axes of the unit has Miller indices (100), (Figure 1.4a, b). an equivalent principles apply to the opposite planes shown. The set of planes that lies parallel to the a- and c-axes, and intersecting the top of every unit at an edge 1 b have Miller indices (010), (Figure 1.4c, d). The set of planes that lies parallel to the a- and b-axes, and intersecting the top of every unit at an edge 1 c have Miller indices (001), (Figure 1.4e, f). Planes cutting both the a-axis and b-axis at 1 a and 1 b are going to be (110) planes, (Figure 1.4 g,h), and planes cutting the a-, b- and c-axes at 1 a, 1 b and 1 c are going to be (111).

Remember that the Miller indices ask a family of planes, not only one . for instance , Figure 1.5 shows a part of the set of (122) planes, which cut the unit edges at 1 a, ½ b and ½ c. The Miller indices for lattice planes are often determined employing a simple method [6].

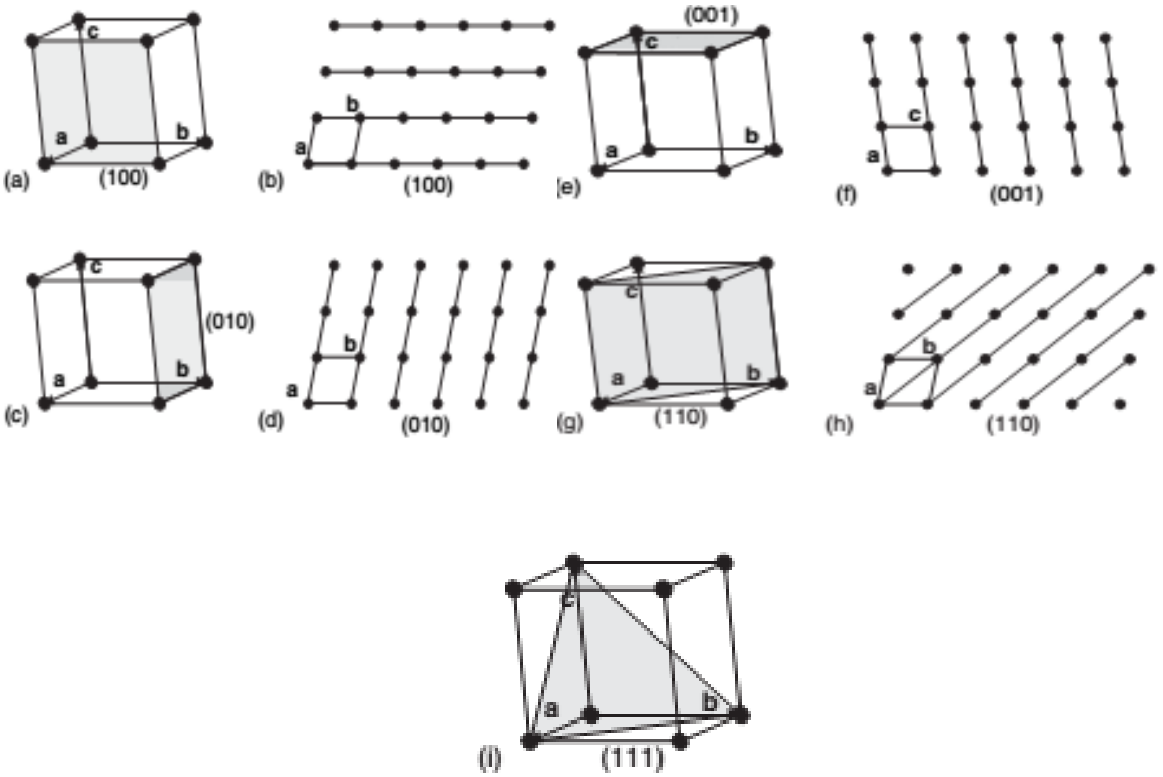

Figure 1.4 Miller indices of lattice planes: (a, b) (100); (c, d) (010); (e, f) (001), (g, h) (110); (i) (111)[6]

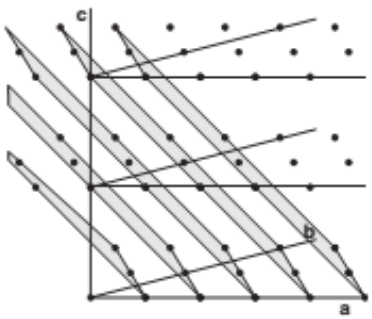

Figure 1.5: Part of the set of (122) lattice planes

The five Bravais lattice that can be received in two-dimension are shown below in fig.1.6*a* along with the primitive cellHere they are described in terms of the elementary translation vectors $\mathbf{a}_1$ and $\mathbf{a}_2$ and of the angle ϕ that they form:

Properties

P1. Squared: $|\mathbf{a}_1| = |\mathbf{a}_2|$ and $\mathbf{a_1}$, $\mathbf{a_2}$ placed at angle $\varphi = \pi/2$

P2. Rectangular: $|\mathbf{a}_1| \neq |\mathbf{a}_2|$, and $\phi = \pi/2$

P3. Body-centered rectangular: As in the rectangular case in P2, but an extra lattice point is located at the canter of each rectangle. Note that this is a cell with two lattice points, located at centre and vertex positions of the rectangle. A cell including more than one lattice site and designed to have all the symmetries of the given lattice is usually named convention a cell. In particular, here the conventional cell is actually not the primitive cell. The latter can instead be represented considering the cell origin at the rectangle centre and choosing a1 and a2 to be the vectors connecting the centre with two vertexes of the same rectangle. In this representation, $|\mathbf{a}_1| = |\mathbf{a}_2|$ but $\phi \neq \pi/2$.

P4. Slanted or oblique: $|\mathbf{a}_1| \neq |\mathbf{a}_2|$and $\phi \neq \pi/2$.

P5. Hexagonal: $|\mathbf{a}_1| = |\mathbf{a}_2|$and $\phi = 2\pi/3$.

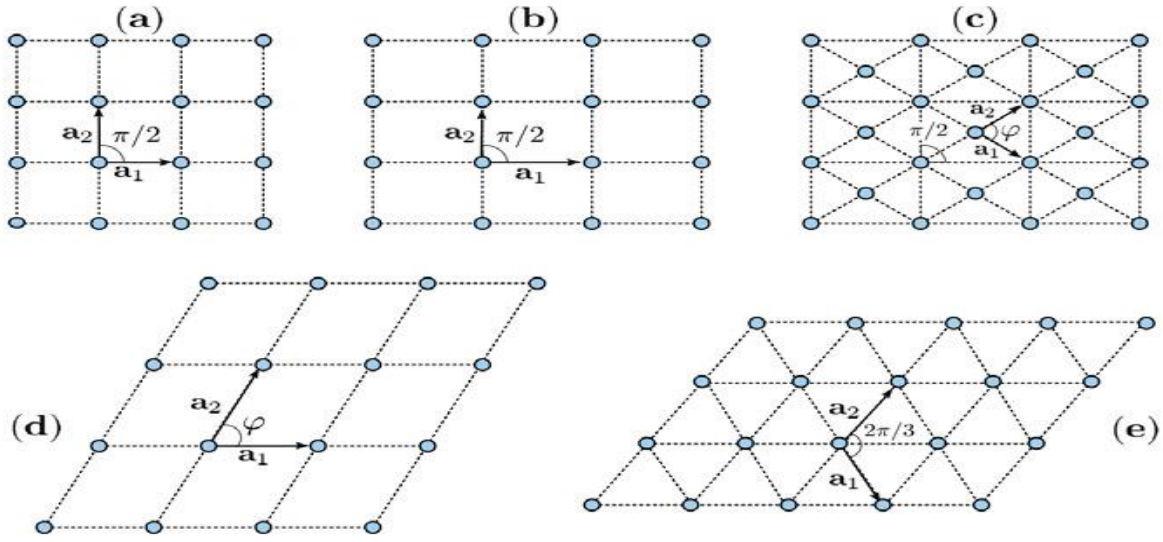

Fig. 1.6: Bravais lattice in 2D. The five conceivable Bravais lattices in 2D are depicted from (a) to (e)[6]

The point-group symmetries related to these 5 lattices are easily picked out. Starting from that with lower symmetry, the slanted lattice in P4 has binary-axes symmetries. To the above binary-axes symmetries, the rectangular P2 and the body-centered rectangular P3 add reflections with respect to the straight-dashed lines in Fig. 1.4 (b) or any other straight line parallel to the latter and crossing at the rectangles centers. The squared lattice in P1 adds quaternary axes symmetries. Finally, the hexagonal P5 has ternary and scenery-axes symmetries, besides reflection symmetries. Note the peculiarity here that two different Bravais lattices, the rectangular and the body-centered rectangular, share the same point-group symmetry.

Three-Dimension Lattice Types

The point symmetry group in thee dimension require the 14 different lattice types listed in Table 1. The general lattice is triclinic, and there are 13 special lattices. These are grouped for convenience into systems classified according to seven types of cells, which are triclinic, monoclinic, orthorhombic, tetragonal, cubic, trigonal, and hexagonal. The division into systems is expressed in the table in terms of the axial relations that describe the cells. The cells in Fig. 6 are conventional cells: of these only the (SC) is a primitive cell. Often a nonprimitive cell has a more obvious relation with the point symmetry operations than has a primitive cell. There are three lattices in the cubic system: the simple cubic (SC) lattice, the body-centered cubic (HCC) lattice, and the face-centered cubic (FCC) lattice

Cubic System

The point-group symmetries are those which leave a cube unchanged and can be counted in the number of 48. Three different Bravais lattices are classified in the cubic system: simple cubic, body-centered cubic and face-centered cubic. All of them are described below, since a great variety of materials occur in either one of these structures.

Tetragonal system

A tetragonal lattice is originated by a cube that is transformed into a parallelepiped with square base. Two different Bravais lattices are classified in the tetragonal system: simple and body-centered tetragonal lattice.

Orthorhombic system

The orthorhombic system is originated from the tetragonal one, after relaxing the requirement that the base be squared. Four different Bravais lattices are classified in the orthorhombic system: simple, base-centered, body-centered, and face-centered orthorhombic lattice.

Monoclinic system

The monoclinic system is originated from the orthorhombic ones, after making the base to be a rhomb. Two different Bravais lattices are classified in the monoclinic system, simple and face-centered.

Triclinic system

The triclinic system is originated from the monoclinic one, after slanting vector $\mathbf{a}_3$ with respect to the direction orthogonal to the plane containing $\mathbf{a}_1$ and $\mathbf{a}_2$.

Trigonal system

The trigonal system is originated from the simple cubic lattice, after deforming the cube along its diagonal: all the faces are rhombus, and each vertex is composed of three corners, each two of them forming the same angle.

Hexagonal system

The hexagonal system is obtained by layering hexagonal lattice planes one on top of the other, at distance *c*. The layering is arranged so that corresponding lattice points in adjacent planes are connected by lines perpendicular to the planes [6].

Table 1.1: Different types of lattice system [1,6]

System	Bravais lattice	unit cell characteristics	Characteristics symmetry elements
Cubic	Simple Body centered Face centered	a = b = c $\alpha = \beta = \gamma = 90°$	Four 3-fold rotation axes (along cube diagonal)
Tetragonal	Simple Body centered	a = b ≠ c $\alpha = \beta = \gamma = 90°$	One fourfold rotation axis
Orthorhombic	Simple Base centered Body centered Face centered	a≠ b ≠ c $\alpha = \beta = \gamma = 90°$	Three mutually orthogonal 2-fold rotation axes.
Monoclinic	Simple Base centered	a≠ b ≠ c $\alpha = \beta = 90° \neq \gamma$	One twofold rotation axis
Triclinic	Simple	a≠ b ≠ c $\alpha \neq \beta \neq 90° \neq \gamma$	None
Trigonal(rhombohedra)	Simple	a = b = c $\alpha = \beta = \gamma \neq 90$	One threefold rotation axis
Hexagonal	Simple	a = b = c $\alpha = \beta = 90$ $\gamma = 120$	One threefold rotation axis

The unit cell of a crystal is defined as that volume of space that its translations allow all the space without intervals and superpositions to be covered. The PUC is the minimal volume

V**a** = $a_1[a_2 \times a_3]$unit cell connected with one Bravais lattice point. Conventional unit cells are defined by two, four and two lattice points, for the base-, face- and body-centered lattices, respectively.\The important characteristics of unit cell of SC, FCC, HCP and diamond cube structure are given below.

Table 1.2: Characteristics of unit cell of different lattices[1,7]

S.N.	Characteristics	SC	BCC	FCC	HCP	DC
1	No of atoms per unit cell	1	2	4	6	8
2	Atomic radius R	a/2	$a\frac{\sqrt{3}}{4}$	$a/2\sqrt{2}$	a/2	$a\frac{\sqrt{3}}{8}$
3	Nearest neighbor distance(2r)	A	$a\sqrt{3}/2$	$a/\sqrt{2}$	a	$\frac{\sqrt{3}}{4}$
4	Coordination no	6	8	12	12	4
5	Unit cell volume	a^3	a^3	a^3	$(a\sqrt{3}/2)a^3$	a^3
6	Packing factor	0.52	0.68	0.74	0.74	0.34
7	Examples	Polonium KCl	Iron Barium, chromium	Al, Cu,Pb Au	Mg , Zn, Cd	Ge , Si, C diamond

Miller indices

All the faces of crystal can be described and numbered in terms of their axial intercepts where, axes represent crystallographic axes which are chosen to fit the symmetry; one or more of these axes may be axes of symmetry or parallel to them, but three convenient crystal edges be used if desire. The intercept *X, Y* and *Z* of this plane on the axes *x, y* and *z* are called parameters ***a, b*** and ***c***. the ratio of parameter ***a: b*** and ***b:c*** are called the axial ratios, and by convention the values of parameters are reduced so that value of b is unity. W. H. Miller suggested in 1839, that each face of crystal could be represented by the indices *h, k* and *l*, defined by [8]

$$h = \frac{\vec{a}}{X}, k = \frac{\vec{b}}{Y}, l = \frac{\vec{c}}{Z}$$

The Reciprocal Lattice

The set of all wave vectors K that yield plane waves with the periodicity of a given Bravais lattice is known as its reciprocal lattice. Analytically, K belongs to reciprocal lattice of Bravais lattice of point R. so we characterize the reciprocal lattice as the set of wave vectors K satisfying

$$e^{iK.R} = 1$$

For all R in Bravais lattice

That the reciprocal lattice is itself a Bravais lattice follow most simply from the definition of Bravais lattice. Let $\mathbf{a_1}$, $\mathbf{a_2}$, and $\mathbf{a_3}$ be a set of primitive vectors for the direct lattice. Then reciprocal lattice can be generated by following three Primitive vectors,

$$\overrightarrow{b_1} = 2\pi \frac{\overrightarrow{a_2} \times \overrightarrow{a_3}}{\overrightarrow{a_1}(\overrightarrow{a_2} \times \overrightarrow{a_3})}$$

$$\overrightarrow{b_2} = 2\pi \frac{\overrightarrow{a_3} \times \overrightarrow{a_1}}{\overrightarrow{a_1}(\overrightarrow{a_2} \times \overrightarrow{a_3})}$$

$$\overrightarrow{b_3} = 2\pi \frac{\overrightarrow{a_1} \times \overrightarrow{a_2}}{\overrightarrow{a_1}(\overrightarrow{a_2} \times \overrightarrow{a_3})}$$

To verify above equation gives a set of primitive vectors for the reciprocal lattice,one first note that the $\mathbf{b_i}$ satisfy

$$b_i . a_j = 2\pi\delta_{ij},$$

Where δ_{ij} is the Kronecker delta symbol.

$$\delta_{ij} = 0, i \neq j,$$

$$\delta_{ij} = 1, i = j,$$

Since the reciprocal lattice is itself a Bravais lattice.

The reciprocal of reciprocal lattice is the set of all vectors **G** satisfying

$$e^{iG.K} = 1$$

For all K in reciprocal lattice,where $K = k_1 b_1 + k_2 b_2 + k_3 b_3$ [9]

The Brillouin zone construction gives the all wave vectors which suffer diffraction from the crystal [10]. The first Brillouin zone has the shape of the truncated octahedron.

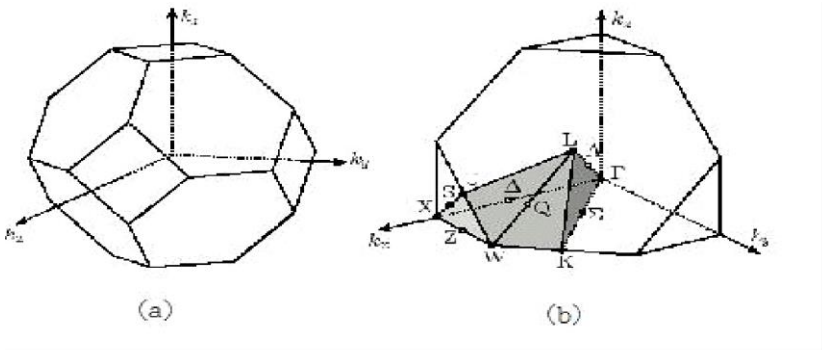

Figure 1.7: Brillouin zone[10]

Density of states

We may find the number of energy levels $dN(E)$ within energy interval E and $E + dE$ (or with n between n and $n + dn$) by counting the number of points that lie in a spherical shell or radius E and thickness dE. It may be noted here that although the energy E (and therefore n) is quantized, the spacing between the successive energy levels becomes infinitesimally small as L becomes large. We can then treat E and therefore n as continuous variables. Then energy interval dE corresponds to an interval dn given by

$$dE = \frac{\hbar^2\pi^2}{2mL^2} \times 2ndn,$$

Now the number of points in the positive octant of a spherical shell of radius n and thickness dn is $dN = \frac{1}{8} \times 4\pi n^2 dn$. we find

$$dN(E) = \frac{1}{4\pi^2}\left[\frac{2m}{\hbar^2}\right]^{\frac{3}{2}} L^3\sqrt{E}dE = \frac{1}{4\pi^2}\left[\frac{2m}{\hbar^2}\right]^{\frac{3}{2}} V\sqrt{E}dE$$

Where, V is the volume of the box (occupied by the system).

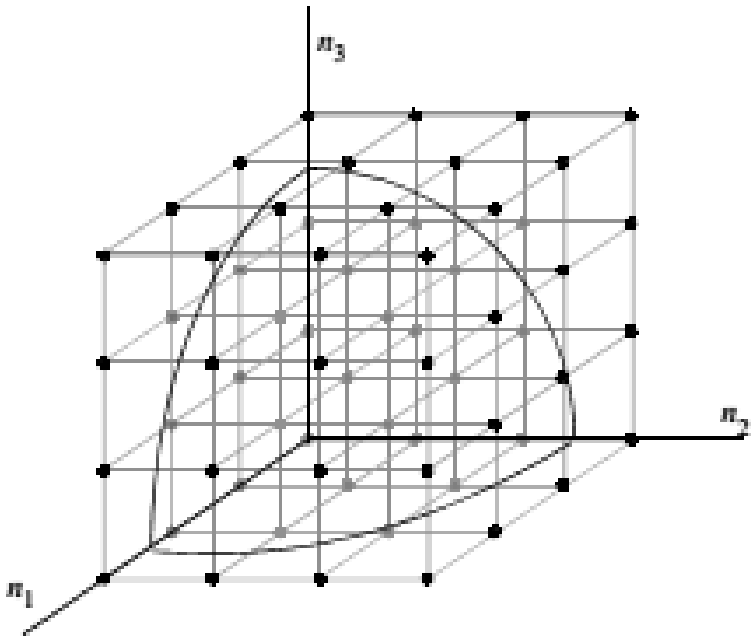

Fig 1.8: When a particle is enclosed in cubical box of dimension L the energy levels are discrete

Each energy state corresponds to a point in three-dimensional (n_1, n_2, n_3)space in the positive octant. The spacing between the successive energy levels can be made as small as desired by choosing *L* sufficiently large [11].

Band Filling and Classification of Materials

One of the great achievement within condensed matter physics during the twenty first cen-tury was the formulation of the Band theory of solid. Categorizing materials based on their electronic transport properties results in three main categories metals, semiconductor and insulators.

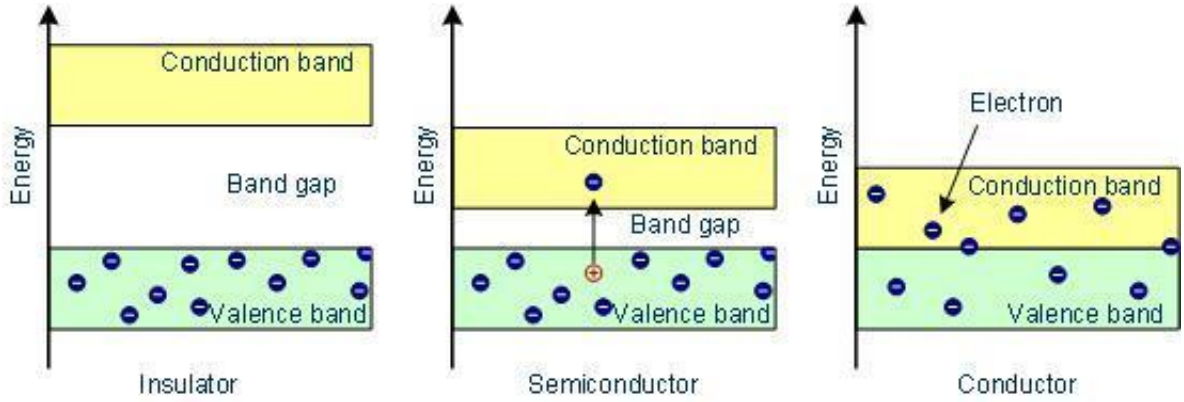

Fig 1.9: Principle sketch of the band structures of insulators, semiconductors and conductors[12]

The semiconductors are defined as insulators with small forbidden gaps. At finite tem-peratures some electrons are excited from the lower valence band to the upper, conduction one. So there are holes in the valence band and the electrons in the conduction one. Such semiconductor is called intrinsic. The modern way to produce materials for electronics is to “dope” semiconductor material with impurity atoms which introduce carriers in a controllable way.The impurity level are usually situated in the forbidden gap. If the impurity levelare situated near the bottom of conduction band the atom are ionized at low enough temperatures and provide extra electrons to the band (such impurities are called donors).Contrary, if the levels are near the top of the valence band they take electrons from the band producing holes (they are called accepters).[13]

If the bans overlap the conduction is usually metallic (Fig. 1.10). Such materials are often called semimetals,if effective number of carriers is small. A typical example of semimetals is Bi.[13]

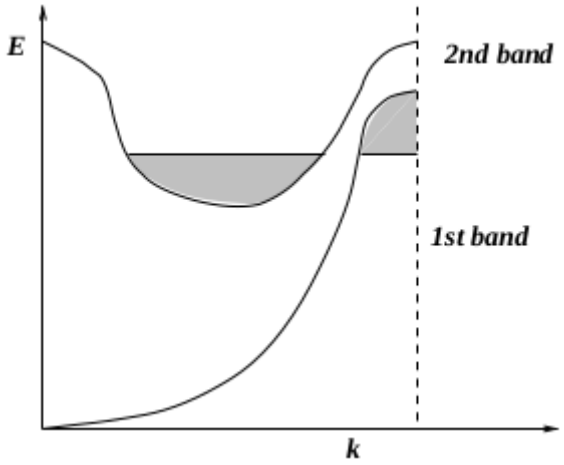

Fig 1.10: The case of band overlap[13]

1.2 Study Material: Antimony and Bismuth

The element Antimony was first observed in compounds and was recorded as a metal at the beginning of the 17th century .Its name was derived from Greek word ‘anti’ means against and ‘monos’ means alone and Stibium in latin.It is a silvery-white brittle solid found in the earth’s crust (0.2 to 0.5 ppm) which is located in Group 15 of the periodic table with nitrogen, phosphrous, arsenic and bismuth.Although antimony resembles a metal it has weak electrical and conductive properties and doesnot shows chemical reaction like a metal and hence classified as semi-metallic[14].

The element Bismuth was discovered by Claude Francois Geoffroy and is derived its name from German word .Bismuth is a brittle white metal with a pinkish tinge which is located in Group 15 of the Periodic table with nitrogen, phosphorus, arsenic and antimony. Bismuth resembles antimony in its mode of occurrence but is less common. The content of bismuth in the earth’s crust has been estimated to be 0.00002 weight %, about the same abundance as silver. Its cosmic abundance is estimated at about one atom per 107 atoms of silicon. The metallic properties of bismuth are more pronounced than that of either antimony or arsenic.In the hydride, BiH_3 bismuth has the compounds of Bi(III) are the most important ones in analytical chemistry.The

compounds of bismuth (V) - alkali metal bismuthates - are known only in the solid state.The ions of bismuth (V) do not exist in solution.Because of its low absorption cross section for thermal neutrons,bismuth has attracted attention as a fuel carrier, and coolant for nuclear reactors [14].

For many years bismuth has attracted the unceasing attention of scientists working in the field of solid-state physics. This is due to its unique electronic properties, which differ considerably from those of common metals. These properties are : (i) low carrier densities (~ 10 ^-5 electrons per atom), (ii) low effective masses (~10^{-1}me, m e being the mass of a free electron), (iii) high diamagnetic susceptibility (~10-~), (iv) high lattice dielectric constant (~ 100), and (v) high values of the g-factor, up to ~ 200.[15]

The knowledge of the atomic electronic properties of As, Sb, and Bi shed light on the electronic properties of their corresponding crystalline state.The external electron configuration of As, Sb, and Bi is S^2p^3 plus a complete d shell. Those s and p levels will mix in the solid, while the other d-electron and core- electron levels will remain practically unchanged. This means that only the five s and p electrons will be considered as valence electrons, while the others will be considered as being part of the ionic core.The s levels lie about 9 eV lower than the p levels.These p levels further split into two levels due to s. o. effects. The amplitude of the p-level splitting increases with the element atomic number: approximately 0. 3 eV for As, 0. 6 eV for Sb, and 1. 5 eV for Bi.[16]

Table 1.3: Some characteristic of element Sb and Bi [14,15,16]

Titles	**Concerned(values ,formulas and others)**	
1. Symbol	**Sb**	**Bi**
2. Group	15	15
3 .Block	p	p
4.Atomic number	51	83
5.Density	6.684 gcm^{-3}	9.78 gcm^{-3}
6.Melting point	630.8°C (1167.44° F)	271.3 °C
7.Boiling point	1587°C (2888.6° F)	1564 °C
8. Relative atomic mass	121.76 amu	208.98038 amu
9.Crystal structure	Rhombohedral,trigonal	Base-centered Monoclinic
10. Electronic Shell structure	2,8,18,18,5	2,8,18,32,18,5
11.Phase	Solid	Solid
12.Colour	Silvery white	Gray
13.Classification	Metalloid	Post-transition metal
14.Electronic Configuration	[Kr] $4d^{10}5s^{2}5p^{3}$	[Xe]$4f^{14}5d^{10}6s^{2}6p^{3}$

1.2.1 Crystal Structure

The group 15 semimetals As, Sb, and Bi have all the same crystal structure, which can be thought of as being composed of two interpenetrating,trigonally distorted,face-centered-cubic lattices.The detailed account crystal structure and its symmetry properties can befound in Brillouin zone.[17]

In fig 1.11 the crystal structure of Sb and Bi,showing first and second neighbors (labeled 1 and 2) to the central atom represented by an open circle.The bisects (C_1),binary(C_2) and trigonal (C_3) axes,and primitive translationvectors (a_1,a_2,a_3) are also shown.

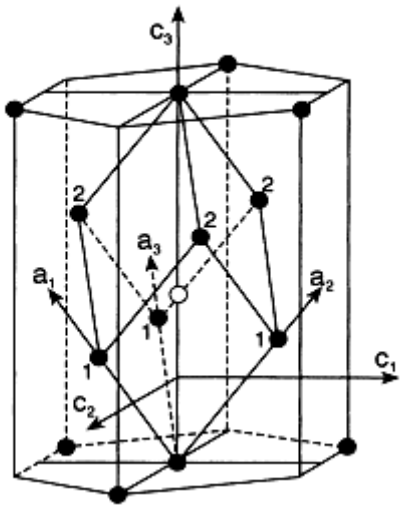

Fig 1.11 :The crystal structure of Sb and Bi[17]

By taking the binary,bisectrix,and trigonal axes to be x,yand z directions respectively.Then the three primitive translation vectors of the lattice are

$$\overrightarrow{a_1} = \frac{-1}{(2a)}, -\frac{\sqrt{3}}{(6a)}, \frac{1}{(3c)}$$

$$\overrightarrow{a_2} = \frac{1}{(2a)}, -\frac{\sqrt{3}}{(6a)}, \frac{1}{(3c)}$$

$$\overrightarrow{a_3} = 0, -\frac{\sqrt{3}}{(3a)}, \frac{1}{(3c)}$$

The three corresponding reciprocal-lattice vectors, defined by

$\mathbf{b_i}.\mathbf{a_j}=2\pi\delta_{ij}$ are given by

$$\overrightarrow{b_1} = \left(-1, -\frac{\sqrt{3}}{3}, b\right) g$$

$$\overrightarrow{b_2} = \left(-1, -\frac{\sqrt{3}}{3}, b\right) g$$

$\overrightarrow{b_3} = \left(0,2\frac{\sqrt{3}}{3}, b\right) g$ where b=a/c.

The relative position of the two basis atoms can written as

d=(0,0,2μ)c

The values of a,c,μand g are listed in below table.

Table 1.4:Crystal structure parameters of Sb and Bi[17,18]

Crystal structure parameters	**symbols**	**Sb**	**Bi**
Lattice constants in hexagonal system	a(A°)	4.3007	4.5332
	c(A°)	11.2221	11.7967
Rhombohedral angle	α	57°14’	57°19’
Internal displacement parameter	μ	0.2336	0.2341
Reciprocal-lattice constant	g(A°)	1.4610	1.3861
Nearest-neighbor distance	d_1(A°)	2.9024	3.0624
Next-nearest-neighbour distance	d_2(A°)	3.3427	3.5120

The A7 structure can be regarded as a distorted cubic structure.It has three nearest neighbors and three second-nearest neighbors.The vectors form a central atom to the nearest neighbors are a_1-d,a_2-d and a_3-d those to the second neighbors are a_1+a_2-d,a_1+a_3-d and a_2+a_3-d.[17]

The minimum energy structure for these elements corresponds to the rhombohedral A**7** structure as *shown* in fig 1.12. This rhombohedral unit cell contains two atoms.It is based on the three vectors starting from the atom labeled O’.In the figure ,the atom labeled A is very close to the center of the cell, but slightly displaced along the trigonal axis of the rhombohedral cell.

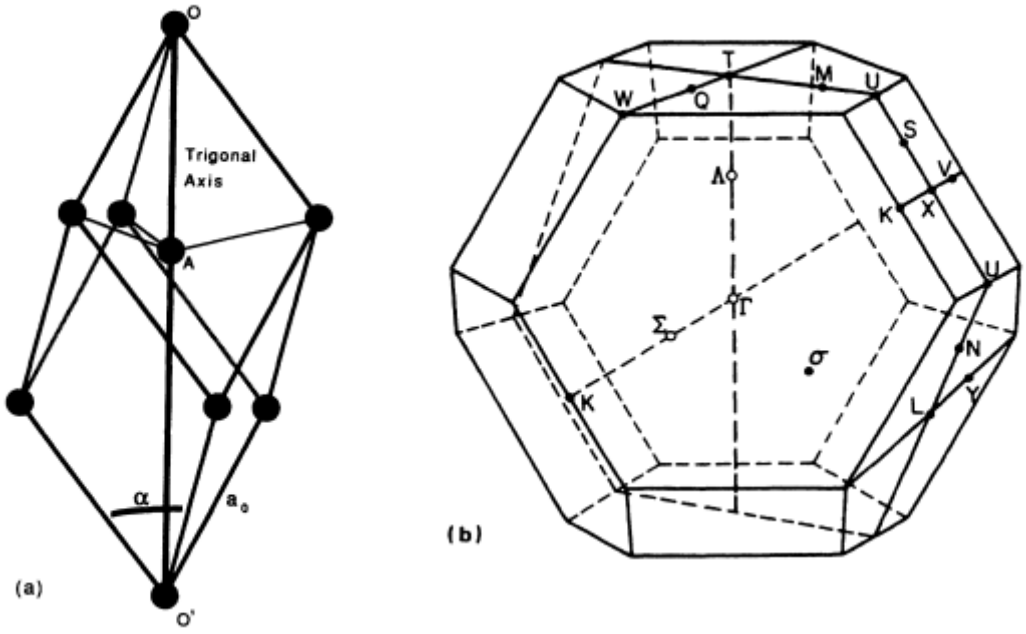

Fig 1.12 :(a) A 7 rhomboedral unit cell (b) The corresponding Brillouin zone.[18]

Centers of inversion are present along the trigonal axis, at the middle of the OA and O'A segments, and at the center of the segments connecting two nearest-neighbor atoms and two next-nearest-neighbor atoms.Three parameters completely determine the unit cell and atom positions: the length ao of the rhombohedral-cell vectors, the rhomboedral angle a, and the position of the second atom along the trigonal axis, determined by the ratio z =OH /OO'. Above table gives these quantities for the two semimetals,and also the nearest-neighbor (NN) distance a NN (or bond length), which increases by about 15% from As to Sb, and by about 5% from Sb to Bi. More details on the A7 structure can be found in Needs at all. These lattice constants and atomic positions will be used in the figure represents the Brillouin zone; the usual notation for symmetry points has been used.[18]

In this present work, we have studies the density of state (DOS) of semimetals antimony and bismuth.From the study of DOS, we can get idea about nature of the solid and magnetic properties. The main objective of our study inciudes the study of crystal structure done by previous researcher and estimate the lattice parameters and observed the nature of plot of density of state of Sb and Bi.

1.3 How we Approach?

Mainly this research work is done is computational by using Quantum ESPRESSO (QE) package. PWscf performs many different kinds of self-consistent calculations of electronic-structure properties within Density-Functional Theory (DFT), using a Plane-Wave (PW) basis set and pseudopotentials (PP).First, we optimized structure of semimetals by optimizing lattice parameters.After that, we study the band structure, DOS and PDOS of Antimony and Bismuth.We use gnuplot for the plotting aspects .

The outline of the present work is summarised follows:

In this paper,Chapter 1 includes theorectical facts i.e. general introduction about crystal structure and lattice dynamics with attachment of objective and scope of work. In chapter 2, we discuss the literature review on semimetals including crystal structure ane pseudopotential.Then, in chapter 3 we explain theoretical models of the method employed in calculations such as Born-Oppenheimer, Hartree-Fock method, Density functional theory with local density approximation (LDA), General gradient approximation (GGA) and Pseudopotential. In chapter 4 we described some detail about Quantum ESPRESSO and its execution. Then in chapter 5 we discuss and present about main calculation and finding of this research. Finally, in chapter 6 we summarize our results and mention about possibilites of further advantage of same field research. Reference are listed at end of chapter 6.

CHAPTER 2

LITERATURE REVIEW

2.1 Introduction and brief review on semi-metals

The structural and electronic properties of the group 15 semi-metals As, Sb and Bi and their alloys have been for many past years the centre of extensive studies.However,these investigations have been either of a complete empirical nature or some based on oversimplified particular models **[20]**.The first successful attempt to find a detailed band structure calculations of this group was carreied out by Falicov and Golin,who determined the structure of arsenic by means of a pseudopotential approach and has been subsequently illustrated by a first principle orthogonalized plane wave calculation,which achieved self -consistency and confirmed the results of Falicov and Golin**[21]**.

It is found that X.Gonze and J.P.Michenaud in 1990 studied the first principles study of As, Sb and Bi electronic properties and explained that these elements crystallize in the rhombohedral A7 structure ,are well known semimetals.Going from top to bottom As to Sb to Bi,the unit cell parameters increaseas well as the strength of the spin -orbit interaction which affecting the quantitative differences in the electronic properties of these materials.They compared the properties of each semimetals such as band structure ,electronic density of charge ,density of states and fermi surfaces with the standard Hohenberg-Kohn-sham density functional approach**[22]**.

Crystalline As,Sb and Bi share two related features i.e. a slight departure from an exact cubic crystallographic structure ,and a weak overlap between valence and conduction bands that leads to a small built in density of free electrons and holes as explained by J.P. Issi,Aust. J. phys in 1979.This latter peculiarity called semimetallic state which leads to an enhancement of many

transport coefficients .Oscillatory phenomena in a magnetic field such as de Haas-van Alphen and Shubnikov de Haas effects ,werw also observed for the first time in Bi**[23]**.

2.2 Crystal structure and pseudopotential

A.ogg in 1922 illustrated the crystalline structure of Antimony and Bismuth.He explained that the antimony crystallises in the dihexagonal alternating (calcite) class of hexagonal crystals. The crystalline symmetry is that of a rhombohedron, the three edges which meet in the trigonal axis being the axes of the crystal.The angle between any two of these edges is 86°58'. From the geometry of the rhombohedral it is easy to find that the angle between the planes (111)and (110) is 87°23' and that between the planes (100) and (111) is 56°48'.Bismuth, like antimony, crystallises in the dihexagonal alternating system (calcite class). The three edges of the rhombohedron meet in the trigonal axis and the angle between any two of the edges is 87°34'. The angle between the faces (100) and (111) is 56°24'.**[24]**

The band structure and fermi surface of semi-metallic Sb are determined by means of pseudopotential approach by L.M.Falicov and P.J.Lin ,department of physics and institute for the study of metals ,the university of chicago Illinoise published in january1966.This paper illustrated the band structure shows three electron pockets located at the point L of the Brillouin zone and six hole pockets with mirror symmetry. The parameters of fermi surface are calculated and comparison with experiment gives good agreement throughout.**[25]**

Since the early 1960s ,a variety of measurements have placed the main features of the band structure and the shape of the fermi surface .From the theoretical point of view band structure and total energy investigations have been carried out.S.Mase,J.phys.soc.japan in 1958 energy mention an early tight-binding calculation for Bi, the qualitative analysis of bonding in group-V rhombohedral compounds, and different semiempirical or approximate studies of As, Sb and Bi.

The investigation of these materials by precise ab initio techniques has only been undertaken recently, and has concentrated mainly on the structural properties.**[26,27]**

Yi Liu and Roland E. Allen developed a third -neighbour tight binding model with spin orbit coupling included to treat the electronic properties of Bi and Sb.This model successfully produces the features near the fermi surface and explained in semimetal-semiconductor device structures,including the small overlap of valence and conduction bands,the electron and hole effective masses and the shapes of the electron and hole fermi surfaces.**[17]**

The calculation of the band structure of antimony was carried out and described the Brillouin zone by showing points, lines, and planes of symmetry.Ninety plane waves were used in the expansion of the pseudowave-functions. Proper factorization of the secular determinant was used at points and lines of symmetry. All the numerical calculations were performed in the BM 7094-7044 system of the University of Chicago Computation Center.The over-all band structure ,position of holes and electron and the approximate position of the Fermi level is marked ,their illustration with experimental result was explained by L.M.Falicov and P. J. Lin.They shown their calculations values of the band energies at the symmetry points T,T y L, and X are given in tabulated form. Also concluded that the Fermi level crosses the bands only near L and T, as expected. The minimum of the sixth band corresponds to the Z 4 level, while the maxima of the fifth band are at six equivalent points called H, which lie on the reflection plane sigma.**[25]**

CHAPTER 3

THEORY

3.1 General consideration

Determination of the electronic structure of solids is a main problem that requires the Schrödinger equation to be solved for an enormous number of nuclei and electrons. Even if we managed to solve the equation and find the complete wave function of a crystal, we face, the some complicated problem of determining how this function should be applied to the calculation of physically observable values. Since the exact solution of the many-body problem is impossible, it is also quite unnecessary.

3.2 Theoretical Details

3.2.1 Born-Oppenheimer approximation

To describe the various motions of the molecule we start with the Schrodinger equation. The Hamiltonian is given by

$$H\hat{} = T\hat{}_e + T\hat{}_N + V_{ee} + V_{eN} + V_{NN}, \tag{3.1.1}$$

Where

$$T\hat{}_e = \sum_{i=1}^{N} \frac{p\hat{}_i^2}{2m} \tag{3.1.2}$$

represents the kinetic energy of the electrons and

$$T\hat{}_N = \sum_{v=1}^{2} \frac{p\hat{}_v^2}{2M_v} \tag{3.1.3}$$

is the kinetic energy of the nuclei. V_{eN} represents the attractive electron-nuclei potential. V_{ee} describes the repelling electron-electron interaction. V_{NN} indicates the repelling Coulomb

interaction between the nuclei. Since the masses of the nuclei are very large,$T\hat{}_N$ can be neglected. This step is called the Born-Oppenheimer approximation. In the following, we will explain the ap- proximation in more detail.

If we neglect the kinetic energy $T\hat{}_N$ of the nuclei (static approximation: fixed distance R of the nuclei), the relative distance R between the nuclei only occurs as a parameter. The Schrodinger equation becomes

$$[e + V_{ee}(r) + V_{eN}(r,R)]\varphi_n(r,R) = [\varepsilon_n(R) - V_{NN}(R)]\varphi_m(r,R). \tag{3.1.4}$$

Here r indicates the position of the electron. The solutions $\varphi_n(r,R)$ depend parametrically on the distance between the nuclei. The energy of this state is given by the electronic energy $\varepsilon_n(R)$ lowered by $V_{NN}(R)$. The solutions $\varphi_n(r,R)$ represent a complete set of functions. The true wavefunction $\psi(r,R)$ can be expanded within this set:

$$\psi(r,R) = \sum_m \quad \phi_m(R)\varphi_n(r,R). \tag{3.1.5}$$

The coefficients $\phi_m(R)$ are to be found and, in general, depend on R. $\varphi_n(r,R)$ is the solution of the full Schrodinger equation, which takes into consideration the kinetic energy $T\hat{}_N$ of the atomic nuclei, i.e.

$$(e + T\hat{}_N + V_{ee} + V_{eN} + V_{NN})\psi(r,R) = E\psi(r,R) \tag{3.1.6}$$

Inserting (2.1.5) into (2.1.6) and using (2.1.4), we obtain

$$\sum_m \quad (\varepsilon_m(R) + T\hat{}_N)\phi_m(R)\varphi_n(r,R) = E\sum_m \quad \phi_m(R)\varphi_m(r,R) \tag{3.1.7}$$

Now we multiply from the left-hand side with $\varphi^{\dagger}{}_n(r,R)$, integrate over the full space, and get

$$\sum_m \quad \int \quad \int \quad d^3r\varphi^{\dagger}{}_n(r,R)T\hat{}_N\phi_m(R)\varphi_m(r,R) + \varepsilon_m(R)\phi_n(R) = E\phi_n(R). \tag{3.1.8}$$

Here we have used the orthogonality of the functions$\varphi_m(r,R)$. $T\hat{}_N$ is proportional to the Laplace operator Δ_R, which acts on $\varphi_m\varphi_m$. It holds that

$$\Delta_R(\phi\varphi) = (\Delta_R\phi)\varphi + 2\Delta_R\Phi.\Delta_R\varphi + \phi\Delta_R\varphi. \tag{3.1.9}$$

The index R indicates the action of the operators in R space. The first term in (3.1.9) is proportional to $T\hat{}_N\phi_n$. The rest is brought to the right-hand side of (3.1.8). The result reads

$$[T\hat{}_N + \varepsilon_n(R)]\phi_n(R) = E\phi_n(R) - \sum_m \quad C_{nm}\phi_m(R) \tag{3.1.10a}$$

With

$$C_{nm}\phi_m(R) = -\hbar^2 \sum_\alpha \quad \frac{1}{2M_\alpha}\int \quad d^3r\varphi^\dagger{}_n(r,R) \times \left[2\nabla_{R_\alpha}\phi_m(R).\nabla_{R_\alpha}\varphi_m(r,R) + \phi_m(R)\nabla_{R_\alpha}\varphi_m(r,R)\right]. \tag{3.1.10b}$$

The sum over a comes from $T\hat{}_N$ and ∇_{R_α}acts only on the co-ordinateR_α of the nucleus α, which appears in $R = \sqrt{(R_2 - R_1)^2}$. Now, the order of magnitude of C_{nm} is $\left(\frac{m}{M}\right)^{\frac{1}{2}}$times smaller than the electronic kinetic energy. This can be seen as follows. The order of magnitude of the term ~ $\hbar^2\nabla_{R_\alpha}\frac{\varphi_m}{2M_\alpha}$ (the kinetic energy of the nucleus) is proportional to $-\left(\frac{m}{M_\alpha}\right)\hbar^2\left(\nabla_r\frac{\varphi_m}{2}m\right)$; we have simply replaced ∇_{R_α} by ∇_r and introduced the electronic kinetic energy $\hbar^2\nabla_{R_\alpha}\frac{\varphi_m}{2M_\alpha}$. The factor m/Ma indicates that the contribution of ∇_{R_α} to C_{nm} is smaller by this factor than the kinetic energy of the electron.

The first term in (3.1.10b) remains to be estimated. For this we approximate ϕ_m by a harmonic oscillator wavefunction: $\phi_m \approx exp$,R_0 being the equilibrium position of nucleus α. We have

$$\nabla_{R_\sigma}\phi_m \approx |R - R_0|\frac{M\omega}{\hbar}\phi_m \approx \frac{(\delta R)M\omega}{\hbar}\phi_m \tag{3.1.11}$$

δRindicates the shift from the equilibrium position. The factor *M* is cancelled by *1/M* in (2.1.10b) and the contribution is proportional to the vibrational energy$\hbar\omega$. As noted earlier, this goes like ~ $\left(\frac{m}{M}\right)^{\frac{1}{2}}$. As a summary, the C_{nm} term can be neglected or treated with the help of perturbation theory. Without the C_{nm} term, (2.1.10a) reduces to

$$[T\hat{}_N + \varepsilon_n(R)]\phi_n(R) = E\phi_n(R) \tag{3.1.12}$$

This equation has an interesting interpretation: the energy of the electron states $\varepsilon_n(R)$ acts like an effective potential in R. We imagine that the electrons build a "medium" in which the atomic nuclei move. This medium acts as an elastic band. If the nuclei try to leave the equilibrium position, they will be drawn back. There is an equilibrium position where $\varepsilon(R)$ has a minimum deep enough to generate binding. The elastic band behaviour is then nothing other than the expansion up to the order $(R - R_0)^2$.

The C_{nm} produce a mixing between different statesφ_n and φ_m. This mixing between the $\varphi_n(R)$ states can be neglected in lowest order, because the C_{nm} are small [of order $\left(\frac{m}{M}\right)^{\frac{1}{2}}$, as explained previously]. Accordingly, the wavefunction is approximately given by

$$\psi_{nv}(r, R) = \phi_{nv}(R)\varphi_n(r, R) \tag{3.1.13}$$

Here v stands for all quantum numbers of level n. E_{nv} indicates the energy of the molecule, which is calculated from (3.1.12).

In order to describe vibrations and rotations of the molecule $\varepsilon_n(R)$ is expanded in coordinates describing vibration and rotation, respectively. The expansion in$\delta R = |R - R_0|$ up to the squared order leads to a harmonic vibrational potential as shown in fig. 2.0. $\varepsilon_N(R)$does not depend on the angles (Euler angles). Hence the rotations of the molecule are free. An excitation of the molecule is a combination of excitations of the harmonic vibrational oscillator and of the rotations.**[28]**

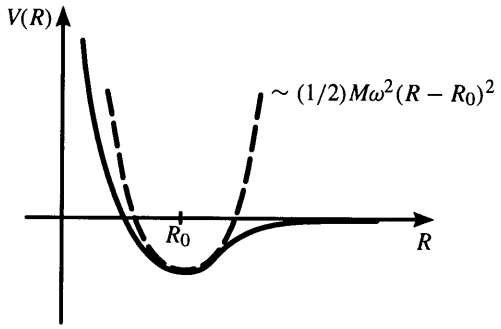

Fig. 2.4: Typical molecular potential for the nuclei in the molecule.Ro characterizes the relative equilibrium position of the two nuclei. R represents the relative nuclear distance[28]

3.2.2 Hartree-Fock Approximation

The simplest approach is to assume a specific form for the many-body wavefunction which would be appropriate if the electrons were non-interacting particles, namely

$$\psi^H(\{r_i\}) = \phi_1(r_1)\phi_2(r_2) \ldots\ldots \phi_N(N) \tag{3.1.14}$$

with the index *i*running over all electrons. The wavefunctions $\phi_i(r_i)$ are states in which the individual electrons would be if this were a realistic approximation. These are single-particle states, normalized to unity. This is known as the Hartreeapproximation (hence the superscript H). With this approximation, the total energy of the system becomes

$$E^H = \langle \Psi^H | H | \Psi^H \rangle$$

$$\sum_i \quad \langle \phi_i \left| \frac{-\hbar^2 \nabla_r^2}{2m_e} + V_{ion}(r) \right| \phi_i \rangle + \frac{e^2}{2} \sum_{ij(j\neq i)} \tag{3.1.15}$$

Using a variational argument, we obtain from this the single-particle Hartree equations:

$$\left[\frac{-\hbar^2 \nabla_r^2}{2m_e} + V_{ion}(r) + e^2 \sum_{j\neq i} \quad \langle \phi_j \vee \frac{1}{|r-r'|} \phi_j \rangle \right] \phi_i(r) + \epsilon_i \phi_i(r) \tag{3.1.16}$$

where the constants $\epsilon_i$are Lagrange multipliers introduced to take into account the normalization of the single-particle states ϕ_i(the bra ϕ_i and ket $|\phi_i >$notation for single-particle states).

Each orbital $\phi_i(r)$ can then be determined by solving the corresponding single-particle Schrödinger equation, if all the other orbitals $\phi_j(r_j), j \neq i$were known. In principle, this problem of self-consistency, i.e. the fact that the equation for one $\phi_i$depends on all the other ϕ_j's, can be solved respectively.

We consider a set of ϕ_i's, use these to construct the single-particle hamiltonian, which allows us to solve the equations for each new ϕ_i we then compare the resulting ϕ_i's with the original ones, and modify the original ϕ_i's so that they resemble more the new ϕ_i's. This cycle is continued until input and output ϕ_i's are the same up to a tolerance δ_{tol}, as illustrated in Fig. 2.2 (in this example, the comparison of input and output wavefunctions is made through the densities, as would be natural in Density Functional Theory, discussed below). The more important problem is to determine how realistic the solution is. We can make the original trial ϕ's orthogonal, and maintain the orthogonality at each cycle of the self-consistency iteration to make sure the final ϕ's are also orthogonal.

Then we would have a set of orbitals that would look like single particles, each $\phi_i(r)$ experiencing the ionic potential $V_{ion}(r)$ as well as a potential due to the presence of all other electrons, $V_i^H(r)$given by

$$V_i^H(r) = +e^2 \sum_{j \neq i} \quad \langle \phi_j \vee \frac{1}{|r-r'|} \phi_j \rangle \tag{3.1.17}$$

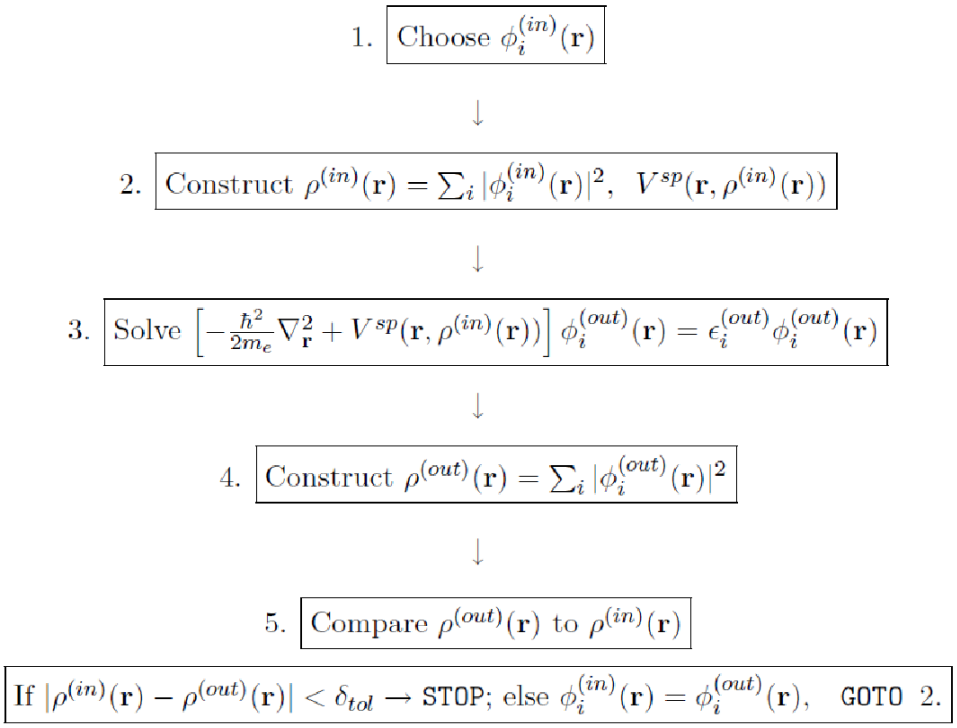

Figure 2.5: Schematic representation of iterative solution of coupled single-particle equations. This kind of operation is easily implemented on the computer

This is known as the Hartree potential and includes only the Coulomb repulsion between electrons. The potential is different for each particle. It is a mean-field approximation to the electron–electron interaction, taking into account the electronic charge only, which is a severe simplification **[29].**

3.2.3 Density Functional Theory

There are numerous fields inside the physical sciences and building where the way to scientific and mechanical advancement is understanding and controlling the properties of issue at the degree of individual iotas and particles. Thickness utilitarian hypothesis is an incredibly best way to deal with finding answers for the essential condition that depicts the quantum conduct of ion as and atoms, the Schrödinger condition, in settings of down to earth esteem. This methodology has quickly developed from being a specific workmanship rehearsed by few physicists and scientific experts at the front line of quantum mechanical hypothesis to a device that is utilized

normally by huge quantities of analysts in science, material science, materials science, substance building, topography, and different controls. A hunt of the Science Citation Index for articles distributed in 1986 with the words "thickness useful hypothesis" in the title or dynamic yields under 50 passages. Rehashing this quest for 1996 and 2006 gives more than 1100 and 5600 passages, separately **[29]**. Right now, start an audit of some key thoughts from quantum mechanics that underlie DFT (and different types of computational science).

The whole field of thickness useful hypothesis lays on two basic numerical hypotheses demonstrated by Kohn and Hohenberg and the inference of a lot of conditions by Kohn and Sham in the mid-1960s **[28]**.The first theorem,proved by Hohenberg and Kohn, is: The ground-state vitality from Schrödinger's condition is a one of a kind utilitarian of the electron thickness.

In spite of the fact that the first Hohenberg–Kohn hypothesis thoroughly demonstrates that a practical of the electron thickness exists that can be utilized to tackle the Schrödinger condition, the hypothesis says nothing regarding what the utilitarian really is. The second Hohenberg–Kohn hypothesis defines a significant property of the practical: The electron thickness that limits the vitality of the general utilitarian is the genuine electron thickness comparing to the full arrangement of the Schrödinger condition. In the event that the "genuine" utilitarian structure were known, at that point we could fluctuate the electron thickness until the vitality from the practical is limited, giving us a solution for finding the significant electron thickness. This variational guideline is utilized by and by with surmised types of the useful.

3.2.4 The Kohn-Sham approach

While the Hohenberg–Kohn theorem rigorously establishes that we may use the density, and and therefore the density alone, as a variable to find the ground-state energy of an N-electron problem, it does not provide us with any useful computational scheme. This is provided by the Kohn–

Sham formalism. Let us then start by considering a noninteracting *N*-electron system in an external potential V_s. The Hamiltonian H_s of this system is given by

$$H_s = T + V_s \tag{3.1.18}$$

We then apply the Hohenberg–Kohn theorem to the present system. Accordingly, there exists a unique energy functional

$$\mathcal{E}_s[n] = T[n] + \int V_s(r)n(r)\,dr \tag{3.1.19}$$

We note here that $T_s[n]$ is the kinetic energy functional of a system of N noninteracting electrons. The ground-state density of this system is easily obtained. It is simply

$$n_s(r) = \sum_{i=1}^{N} |\phi_i(r)|^2 \tag{3.1.20}$$

where we have occupied the N single-particle states, or orbitals, that satisfy the Schrödinger-like equation

$$\left[\frac{-\hbar^2}{2m}\nabla^2 + V_s\right]\phi_i(r) = \mathcal{E}_i\phi_i(r), \mathcal{E}_1 \leq \mathcal{E}_2 \leq \mathcal{E}_3 \ldots, \tag{3.1.21}$$

and have the *N* lowest eigenvalues $\mathcal{E}_i$. But we are really interested in a system of *N* interacting electrons in an external potential V_{ext}, so the question we would like to answer is the following: can we determine the form that V_s (the external potential of the noninteracting system) must take in order for the noninteracting system to have the same ground-state density as the interacting system in the external potential V_{ext}? The strategy we use is to solve for the density using the auxiliary noninteracting system, and then insert this density (which by construction is the same as that for the interacting system) into an approximate expression for the total energy of the interacting system. The first step in this process is to rewrite the energy functional $\mathcal{E}[n]$ of the interacting system, which was given in Eq. (3.1.21), as

$$\mathcal{E}[n] = T_s[n] + \left\{T[n] - T_s[n] + V[n] - \frac{e^2}{2}\iint \frac{n(r)n(r')}{|r-r'|}drdr'\right\} + \frac{e^2}{2}\iint \frac{n(r)n(r')}{|r-r'|}drdr'$$

$$+ \int n(r)V_{ext}(r)dr$$

$$\equiv T_s + \frac{e^2}{2}\iint \frac{n(r)n(r')}{|r-r'|}drdr' + \iint n(r)V_{ext}(r)dr + \mathcal{E}_{XC}[n], \quad (3.1.22)$$

Here we have added and subtracted both the kinetic energy functional $T_s[n]$ of a noninteracting system and the direct, or Hartree, term in the electrostatic energy. We have then defined the sum of the terms in braces to be the exchange-correlation energy functional $\mathcal{E}_{XC}[n]$ is

$$\mathcal{E}_{XC}[n] \equiv F_{HK}[n] - \frac{e^2}{2}\iint \frac{n(r)n(r')}{|r-r'|}drdr' - T_s[n], \quad (3.1.23)$$

We have thus swept all our ignorance about electron interactions beyond the Hartree term under the rug that we call $\mathcal{E}_{XC}[n]$. What we gain in writing $\mathcal{E}_{XC}[n]$ this way is that we can eventually focus on developing reasonable approximations for $\mathcal{E}_{XC}[n]$. According to the Hohenberg–Kohn theorem, the density n that minimizes the functional $\mathcal{E}[n]$ is the ground-state density. Thus, by taking the variation of Eq. (2.1.22) with respect to the particle density we obtain

$$\frac{\delta\mathcal{E}[n]}{\delta n(r)} = \frac{\delta T_s[n]}{\delta n(r)} = e^2\int \frac{n(r')}{|r-r'|}dr' + V_{ext}(r) + v_{xc}[n(r)] = 0, \quad (3.1.24)$$

where we have formally defined the exchange-correlation potential as

$$v_{xc}[n(r)] \equiv \frac{\delta\mathcal{E}_{xc}[n]}{\delta n(r)}.$$

We now use the auxiliary noninteracting system and its Schrödinger equation, from which we are able to similarly show that

$$\frac{\delta T_s[n]}{\delta n(r)} + V_s(r) = 0.$$

By comparing this result with Eq. (2.5.6) we see that this ejective potential V_s (r) must satisfy

$$V_s(r) = V_{ext}(r) + e^2 \int \frac{n(r')}{|r-r'|} dr' + v_{xc}(r), \qquad (3.1.25)$$

We are now doing a position to implement the self-consistent Kohn–Sham scheme. We first choose an initial trial form of the function $n(\mathbf{r})$ and substitute into Eq. (3.1.25) to find a trial form of V_s. We then solve Eq. (3.1.19) for the single-particle wavefunctions$\phi_i(r)$, and use Eq. (3.1.18) to find the next iteration for $n(\mathbf{r})$. When this procedure has been repeated a sufcient number of times that no further changes occur, then a solution for $n(\mathbf{r})$ has been found that not only satisfies the Schrödinger equation for the reference noninteracting electrons, but also is the correct density for the interacting system. We close this section by highlighting a few points about the Kohn–Sham formalism. First of all, it is formally exact, supposing that we can find the exact exchange-correlation potential $v_{xc}(r)$. Second, we have cast the solution of the interacting N-electron problem in terms of noninteracting electrons in an external potential $V_s(r)$. This is of great practical importance. The ground state wavefunction of the noninteracting system is just a Slater determinant of the N orbitals, the so-called Kohn–Sham orbitals, with the lowest eigenvalues E **[30]**. It is relatively easy to unravel for these single-particle orbitals even for as many as a couple of hundred electrons. The Kohn–Sham equations formally look considerably like self-consistent Hartree equations, the only difference being the presence of the exchange-correlation potential which makes them much simpler to solve than the Hartree–Fock equations, in which the potential is orbital-dependent. In the Kohn–Sham and Hartree equations, the effective potential is the same for every orbital.

3.2.5 The Local Density Approximation

In band calculations, usually certain approximations for the exchange–correlation potential $V_{xc}(r)$ are used. The simplest and most frequently used is the local density approximation (LDA), where $\rho_{xc}(r, r'-r)$a form similar to that for a homogeneous electron has gas, but with the density at

every point of the space replaced by the local value of the charge density, $\rho(r)$for the actual system:

$$\rho_{xc}(r, r' - r) = \rho(r) \int_0^2 \quad d\lambda g_0\big(r - r' \vee, \lambda, \rho(r)\big) - 1, \tag{3.1.26}$$

Where,g_0 is the pair correlation function of a homogeneous electron system. Substituting (3.1.26) into (3.1.27) we obtain the local density approximation [44]:

$$E_{xc}[\rho] = \int \rho(r)\varepsilon_{xc}(\rho)\, dr, \tag{3.1.27}$$

Here, ε_{xc} is the contribution of exchange and correlation to the total energy (per electron) of a homogeneous interacting electron gas with the density$\rho(r)$. This approximationcorresponds to surrounding every electron by an exchange– correlation hole and must, as expected, be quite good when $\rho(r)$varies slowly. The DFT includes the exchange and correlation effects in a more natural way in comparison with Hartree-Fock-Slater method. Here, the exchange– correlation potential V_{xc} may be represented as

$$V_{xc}(r) = \beta(r_e)V_{GKS}(r), \tag{3.1.28}$$

where V_{GKS} is the Gaspar–Kohn–Sham potential, and r_e is given by

$$r_e(r) = \left[\frac{3}{4\pi}\rho(r)\right]^{\frac{1}{3}}. \tag{3.1.29}$$

This parameter corresponds, in order of magnitude, to the ratio of the potential energy of particles to their average kinetic energy.

3.2.6 The Generalized Gradient approximation

An early endeavor to improve the LSDA was the inclination development estimation (GEA). Figurings for molecules and a jellium surface appeared, be that as it may, that the GEA doesn't improve the LSDA if the stomach muscle initio coefficients of the slope revision are utilized. The blunders in the GEA were examined by Langreth and Perdew and later by Perdew and

colleagues. It was demonstrated that the second request developments of the trade and relationship openings in angles of the thickness are genuinely sensible near the electron, yet not far away. In the first work of Langreth and associates a summed up inclination guess (GGA) was developed by means of cut-off of the deceptive little wave-vector commitment to the Fourier change of the second request thickness angle extension for the trade relationship opening around an electron. Later Perdew and associates contended that the inclination developments can be made increasingly practical by means of genuine space shorts picked to authorize careful properties regarded by zero-request or LSD terms however abused constantly request extensions: The trade gap is rarely positive, and incorporates to - 1, while the relationship opening coordinates to zero. Various GGA plans were created by Langreth and Mehl, Hu and Langreth (LMH), Becke, Engel and Vosko, and Perdew and collaborators (PW), the three best and well known ones are those by Becke (B88), Perdew and Wang (PW91), and Perdew, Burke, and Ernzerhof (PBE). In GGA the trade relationship utilitarian of the electron turn densities $\rho_{\uparrow}$ and $\rho_{\downarrow}$ takes the form

$$E_{xc}^{GGA}[\rho_{\uparrow}, \rho_{\downarrow}] = \int \quad d^3rf(\rho_{\uparrow}, \rho_{\downarrow}, \nabla\rho_{\uparrow}, \nabla\rho_{\downarrow}) \tag{3.1.29}$$

The GGA functionals were tried in a few cases, and were found to give improved outcomes for the ground-state properties. For iotas it was discovered that both all out energies and expulsion energies are improved in the LMH practical contrasted and the LSDA. The PW practical gives a further improvement in the all out vitality of iotas. The coupling energies of the first push diatomic atoms are additionally improved by both functionals. In an investigation of the band structure of V and Cu, Norman and Koelling found that the LMH potential gave an improvement in the Fermi surface for V yet not for Cu. The strong vitality, the cross section parameters, and the mass modulus of third-push components have been determined utilizing the LMH, PW, and the angle extension functionals in. The PW practical was found to give to some degree preferred outcomes over the LMH utilitarian and both were found to commonly evacuate a large portion of

the mistakes in the LSD estimate, while the GEA gives more terrible outcomes than neighborhood thickness guess. For Fe GGA functionals accurately anticipate a ferromagnetic bcc ground state, while the LSDA and the angle extension foresee a nonmagnetic FCC ground state. Likewise, the GGA amends LSDA underestimation of the cross section constants of Li and Na. Enormous number of test estimations demonstrated that GGA functionals yield incredible improvement over LSD in the portrayal of finite frameworks: they improve the complete energies of particles and the strong vitality, harmony separation, and vibrational recurrence of atoms, however have blended history of achievements and disappointments for solids. This might be on the grounds that the trade connection opening can have a diffuse tail in a strong, yet not in a particle or little atom, where the thickness itself is all around confined. The general pattern is that the GGA thinks little of the mass modulus and zone focus transverse optical phonon recurrence, remedies the coupling vitality, and amends or overcorrects, particularly for semiconductor frameworks, the cross section consistent contrasted with LDA. The GGA doesn't take care of the issues experienced in the change metal monoxides FeO, CoO, and NiO. The attractive minutes and band structures acquired with the GGA for the oxides are basically indistinguishable off base ones from got with the LSDA. As of late, various endeavors have been made to broaden the GGA by including higher request terms, specifically the Laplacian of the electron thickness, into the extension of the trade connection gap. Be that as it may, no broad trial of the nature of these new possibilities with application to solids have yet been made **[31]**.

3.3 Pseudo-potentials

Pseudopotential is the essential application in electronic structure is to supplant the solid Coulomb capability of the core and the impacts of the firmly bound center electrons by a powerful ionic potential following up on the valence electrons.It can be created in a nuclear estimation and afterward used to process properties of valence electrons in atoms or solids, since the center states remain practically unaltered. Moreover, the way that pseudopotentials are not

special permits the opportunity to pick shapes that disentangle the computations and the translation of the subsequent electronic structure. The approach of "stomach muscle initio standard saving" and "ultrasoft" pseudopotentials has prompted precise estimations that are the reason for a great part of the momentum innovative work of new techniques in electronic structure, as portrayed in the accompanying sections. A large number of the thoughts started in the orthogonalized plane wave (OPW) approach that throws the eigenvalue issue as far as a smooth piece of the valence capacities in addition to center (or center like) capacities. The OPW technique has been brought into the advanced system of all out vitality functionals by the projector increased wave (PAW) approach that utilizations pseudopotential administrators yet keeps the full center wavefunctions.

a)Norm-conserving pseudopotentials

Pseudopotentials generated by calculations on atoms (or atomic-like states) are termed "ab initio" because they are not fitted to experiment. The concept of "norm-conservation" has a special place in the development of ab initio pseudopotentials; at one stroke it simplifies the application of the pseudopotentials and it makes them more accurate and transferable. Norm-conserving pseudofunctions$\psi_{ij}(r)$ are normalized and are solutions of a model potential chosen to reproduce the valence properties of an all electron calculation. In the application of the pseudopotential to complex systems, such as molecules, clusters, solids, etc., the valence pseudofunctions satisfy the usual orthonormality conditions as

$$\langle \psi_i^{\sigma,PS} \vee \psi_i^{\sigma',PS} \rangle = \delta_{i,j}\delta_{\sigma,\sigma'} \tag{2.1.31}$$

so that for the Kohn-Sham equations have the same form as

$$\left(H_{KS}^{\sigma,PS} - e_i^{\sigma}\right)\psi_i^{\sigma,PS}(r) = 0 \tag{2.1.32}$$

b) Ultrasoft pseudopotential (USPP)

One goal of pseudopotentials is to create pseudofunctions that are as "smooth" as possible, and yet are accurate. "Norm-conserving" pseudopotentials achieve the goal of accuracy, usually at some sacrifice of "smoothness."

A different approach known as "ultrasoft pseudopotentials" reaches the goal of accurate calculations by a transformation that re-expresses the problem in terms of a smooth function and an auxiliary function around each ion core that represents the rapidly varying part of the density. We will focus upon examples of states that present the greatest difficulties in the creation of accurate, smooth pseudofunctions: valence states at the beginning of an atomic shell, *Is,2p, 3d,* etc.

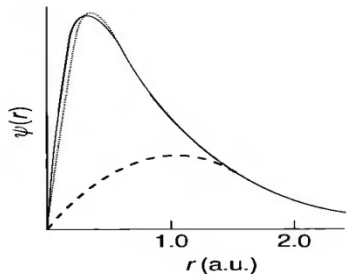

Figure 2.6: 2p radial wavefunction$\psi(r)$ for oxygen treated in the LDA, comparing the all-electron function (solid line), a pseudofunction generated using the Hamann approach (dotted line), and the smooth part of the pseudofunction$\tilde{\psi}$ in the "ultrasoft" method (dashed line).

For these states, the OPW transformation has no effect since there are no core states of the same angular momentum. Thus, the wavefunctions are nodeless and extend into the core region. Accurate representation by norm-conserving pseudofunctions requires that they are at best only moderately smoother than the all-electron function (see Fig.2.3) The difference in the norm

equation $Q_l = \int_0^{R_c} \quad dr\phi_l(r)^2$from that norm-conserving function $\phi = r\psi\sim$ (either an all-electron function or a pseudofunction) is given by

$$\Delta Q_{s,s\prime} = \int_0^{R_c} \quad dr\Delta Q_{s,s'}(r). \tag{2.1.33}$$

Where

$$\Delta Q_{s,s'}(r) = \phi_s\ (r)\phi_{s'}(r) - \phi\sim_s\ (r)\phi\sim_{s'}(r). \tag{2.1.34}$$

A new non-local potential that operates on the $y can now be defined to be

$$\delta V\hat{}_{NL}^{US} = \sum_{s,s\prime} \quad D_{s,s\prime} \vee \beta_s > \beta_{s\prime} \vee, \tag{2.1.35}$$

Where

$$D_{s,s'} = B_{s,s'}\varepsilon_{s'}\Delta Q_{s,s'}. \tag{2.1.36}$$

For each reference atomic states *s*, it is straightforward to show that the smooth functions $\psi\sim_s$are the solutions of the *generalized eigenvalue problem*

$$[H\hat{} - \varepsilon_s S\hat{}]\psi\sim_s = 0, \tag{2.1.37}$$

With$H\hat{} = \frac{-1}{2}\Delta^2 + V_{local} + \delta V\hat{}_{NL}^{US}$ and $S\hat{}$ an overlap operator,

$$S\hat{} = 1\hat{} + \sum_{s,s\prime} \quad \Delta Q_{s,s'}|\beta_s > \beta_{s'}|, \tag{2.1.38}$$

which is different from unity only inside the core radius. The eigenvalues ε_s agree with the all-electron calculation at as many energies s as desired. The full density can be constructed from the functions $\Delta Q_{s,s'}(r)$, which can be replaced by a smooth version of the all-electron density. The advantage of relaxing the norm-conservation condition $\Delta Q_{s,s'} = 0$ is that each smooth pseudofunction $\psi\sim_s$ can be formed independently, with only the constraint of matching the value of the functions $\psi\sim_s(R_c) = \psi_s(R_c)$ at the radius R_c. Thus, it becomes possible to

choose R_c much larger than for a norm-conserving pseudopotential, while maintaining the desired accuracy by adding the auxiliary functions $\Delta Q_{s,s'}(r)$ and the overlap operator S. An example of the un-normalized smooth function for the 2p state of oxygen is shown in Fig. 2.9.1, compared to a much more rapidly varying norm-conserving function **[32]**

3.4 Band Structure

If we knew the potential $V_P(r)$, and could solve the one-electron Schrödinger equation

$$\frac{-\hbar^2}{2m_e}\nabla^2\psi(r) + V_P(r)\psi(r) = E\psi(r)$$

we could ascertain the energies E of the entirety of the different potential states. There are a few different ways of moving toward such figurings from first standards, and we won't go into those here. The after effects of such counts give what is known as a band structure. The electronic conditions of precious stones are portrayed by the band hypothesis of solids. The external orbital's of the molecules in a thickly stuffed strong cover with one another as the synthetic bonds that hold the gem together are framed. This causes the discrete vitality levels of the free ion as to be expanded into groups. The differentiation between a protector and a semiconductor is identified with the size of the band gap. Semiconductors have littler band holes than encasings. The free electrons in the conduction band can direct power effectively in a similar way as the free electrons in metals. Semiconductors, hence, have a higher conductivity than encasings, yet a littler conductivity than metals as a result of the modest number of free electrons **[33]**. There are various groups in a band structure (in actuality a limitless number), yet generally, just a couple are significant in deciding specific properties of a material. Fig. 8.4 outlines a basic band structure. Each band has an all outnumber of permitted k-states equivalent to the number of unit cells in the precious crystal.

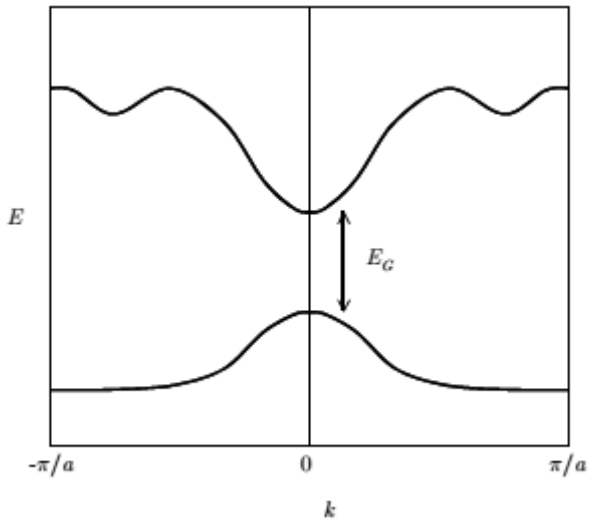

Fig. 2.7: Figurative illustration of a semiconductor band structure, plotted along one crystal direction. The upper "band" (line) will be essentially empty of electrons, and is called the conduction band; the lower band will be essentially full of electrons, and is called the valence band.

Fig. 2.4 illustrates a simplified band structure. In each band, we only have to plot *k*-values from $-\pi / a$ to π / a. The band structure in Fig. 2.4 is also drawn to be symmetric about $k = 0$. Band structures are often symmetric in this way. In our simple one-electron model, neglecting magnetic effects, the existence of symmetries like this is easily proved **[34]**.

3.5 GW approximation

While we have given some justifications to utilizing a straight forward LSDA band structure way to deal with assessing excitation energies, various materials with intriguing attractive properties include firmly corresponded electronic states, and other estimated approaches have been created to go past the LSDA. For the quasiparticle issue, the focal issue is a sufficient estimation for the self-vitality administrator, $\Sigma_{GW}(r, r'; E)$. A working technique for tackling this issue is the purported GW estimation. On the off chance that the pinnacle is sufficiently sharp, well-defined quasiparticle vitality can be acquired. Where the self-energy is

$$\Sigma_{GW}(r,r';t) = iG(r,r';t)W(r,r':t) \tag{2.1.39}$$

The self-vitality in the GW A has a similar structure as that in the Hartree-Fock estimate aside from that it relies upon the vitality and contains a term that relies upon abandoned states as an outcome of relationship impacts. In this manner, the GW A can be deciphered as a speculation of the Hartree-Fock estimate with a potential that contains dynamical screening of the Coulomb potential. The GWA has been fruitful in treating the quasiparticle frameworks, for example, free-electron like metals and semiconductors It can be demonstrated that the GWA hypotheses might be identified with a Hartree-Fock hypothesis with a recurrence and orbital-subordinate screened Coulomb association and, at any rate for confined states, for example, d or f orbital's of progress metal or uncommon earth metal particles **[35]**.

CHAPTER 4

COMPUTATIONAL DETAILS

4.1 General Consideration

Our present work with the first principle pseudopotential-based density functional calculations including norm-conserving pseudo-potential in the DFT approach by using the quantum ESPRESSO (QE) computational package and some practicable commands along with their functions are well detailed here.

4.2 Quantum Espresso Program

In this program,we can use the Density Functional Theory (DFT) to investigate the properties of different materials. DFT is broadly utilized in industry, and in the scholastic research network since it is one of the computational techniques that can (roughly) tackle reasonable quantum mechanical issues numerically. Quantum ESPRESSO-a condensing for Quantum Open-Source Package for Research in Electronic Structure, Simulation, and Optimization program is a multi-reason and multi-stage PC coding program for electronic-structure figurings and materials demonstrating**[35]**. This bundle is essentially utilized in the stomach muscle ab-initio estimations of dense issue frameworks. In a controlled issue material science, its ordinary application in the stomach muscle ab-initio estimations like-basic advancements (both at zero and limited temperature), direct reaction computations (Phonons, flexible constants, dielectric, and some more) and so forth stretches out to high-temperature atomic elements. The significant element of the bundle remembered for the product are as follows:

a) Plane Wave self-consistent field (PWscf)

b)First-Principles Molecular Dynamics (FPMD) and

c)Car-Parrinello (CP). QE, based on DFT, implements a variety of methods and

algorithms for a chemically realistic modelling of materials from the Nanoscale upwards

d) Chemical reactivity and transition-path sampling, using Nudged Elastic Band (NEB)method.

e)Computational microscopy (STM). This package uses a plane waves (PWs) basis set for the expansion of electronic wave function, a pseudopotentials (PPs) to represent electron-ion interactions and DFT for the description of electron-electron interaction.

Some basic computations/simulations that can be performed by this package include:

- Calculations of the Kohn-Sham (KS) orbitals and energies for isolated and extended systems, and of their ground states energies.
- Structural modelling (equilibrium structures of molecules, crystals, surfaces).
- Atomic forces and stresses.
- Ground state studies of magnetic or spin-polarized systems.
- Dynamical modeling (first-principles molecular dynamics) either in the electronic ground state (Born-Oppenheimer) or with fictitious electronic kinetic energy (Car-Parrinello).

Density-Functional Perturbation Theory (DFPT) used in the package to calculate the energy derivatives and related quantities. QE package are used as our first -principles code. QE is a full ab- initio package implementing electronic structure and energy calculation, linear response method (to calculate dielectric constants, Born effective charge and phonon dispersion curves) and third order an-harmonic perturbation theory. It also contains two molecular- dynamics codes, CPMD (Car-Parrinello Molecular Dynamics) and FPMD (First-Principles Molecular Dynamics). Among them, to perform the total energy calculations, PWscf code is used, which

used both norm-conserving pseudopotential (PP) and Ultra soft Pseudo-potentials (US-PP) within DFT. In our case, we use Quantum ESPRESSO integrated module of codes, based on DFT by using plane basis set for expansion of wave function and pseudopotential with required content in first-principle method of calculation to calculate total energies and optimize geometries of semi-metals Sb and Bi. Also, by using this package, band structure is calculated and partial density of states (PDOS) is used to find the nature of material.

4.2.1 PWscf

PWscf stands for Plane Wave self-consistent field (which in earlier releases included PHonon and PostProc), developed by Stefano Baroni, Stefano de Gironcoli, Andrea Dal Corso (SISSA) Paolo Giannozzi (Univ. Udine) and many others**[36]**.

PWscf implementsan iterative approach for self-consistency, in the framework of the plane-wave pseudo potential method. This package uses the well-established LDA and GGA exchange-correlation functionals, including spin-polarizations. The main feature of PWscf calculation is the self-consistency calculations, structural relaxation, electronic structure calculations, variable cell molecular dynamics calculation, etc, performed by invoking executable file called **pw.x**. The structural optimization is performed using the Broyden-Fletcher-Goldfarb-Shanno (BFGS) **[36,37]**.

Some of the most important parameters in the input file of the Quantum espresso are as indicated below.

- &CONTROL: general variables controlling the run
- &SYSTEM: structural information on the system under investigation
- &ELECTRONS: electronic variables: self-consistency, smearing
- ibrav : 4 for Sb, this keyword generates hexagonal closed pack (hcp) structure and 0 for Bi.

- celldm(1): specifies the lattice constant of the crystal and are usually given in atomic unit.
- ecutwfc: kinetic energy cutoff (Ry) for wavefunctions (1 Ry=13.6ev).
- nat: number of atoms in the unit cell.
- ntyp: number of types of atoms in the unit cell.
- nbnd: represents the number of electronic stated (bands) to be calculated.
- Atomic Species: It specifies the symbols of the atoms, their corresponding masses (in amu) and the name of the files containing the pseudo-potentials.
- Atomic Positions: specifies the atomic co-ordinates of the atoms which are defined for the proper structure.
- k-points: represents the rectangular grid of points of dimensions, spaced evenly throughout the Brillouin zone and this keyword requires appropriate unit.

4.2.2 Post Processing

The package called Postprocessing was Originally developed by Stefano Baroni, Stefano de Gironcoli, Andrea Dal Corso (SISSA), Paolo Giannozzi (Univ. Udine), and many others. After the Self Consistent calculation has been converged, we use many small calculations such as plotting of band, density of states (DOS) etc. The main post processing codes which extract the specified data/files from the PWscf calculations and perform further calculations are as follows:

• **pw.x:** This command is used to run the input files of scf and nscf calculations of energy and wave functions at each k-points, which extracts the output files for the energy calculation at every k-points.

• **bands.x** : This extracts the files from PWscf calculation and records its eigenvalues at different K-points with corresponding energies values ready for further processing. The code **bands.x** also performs the symmetry analysis of the band structure.

•**plotband.x** : The output file of **bands.x** is directly read and converted to plottable format by auxiliary code **plotband.x**. The value of k-points must be correctly put in a sequence, otherwise unpredictable plots may result if k-points are not in sequence along lines or if two consecutive points are same.

• **dos.x**: This code helps us to calculate the electronic density of states at different k-points.
•**projwfc.x**: This code calculates projections of wave functions over atomic orbitals. It gives the contributions of the atomic orbitals s, p, d, f.

4.3 Gnuplot

Gnuplot is a fairly small, mature, general-purpose plotting program.Advantage of using Gnuplot to display the orbitals is that the skills learned to master the program may be useful for other purposes, such as displaying data from a lab report.The simple syntax for specifying a plot in Gnuplot means that writing a plotting file for an orbital is simply a matter of transcribing the analytical form of the function to be plotted.or complicated plots, the best way to proceed is to save a series of plot commands in a text file. The command file may be edited with any text editor (the vi or emacs editor on a UNIX system, Notepad on a PC/Windows system, etc.).For example, if we have saved a text file of Gnuplot commands named plotfig.gnu , then at the Gnuplot command prompt we would type the command load "plotfig.gnu" .The quotes are required. Filenames are specified in quotes in Gnuplot.The specifics of the appearance of the plots produced by Gnuplot are dependent on the display device. To achieve a consistency of output format in a reasonably portable form,I have chosen for this paper to use Gnuplot's postscript driver.All the experimental results optimaization results ,bands,dos,pdos are shown in graphical plot by using script of gnuplot **[38]**.

CHAPTER 5

RESULTS AND DISCUSSION

5.1 General Consideration

This thesis has describes the comparative study of element antimony (Sb) and bismuth (Bi).One of the main challenges in first principle calculation is the geometric optimization of structures. We have taken out the energy minimization of Sb and Bi, followed by the study of electronic band structures and the density of states. The calculation has been carried out using density functional theory using generalized gradient approximation. At first, in the GGA method, energy minimization is done with respect to the lattice parameter then the same lattice parameter corresponding to the minimum energy state is used to carry out further calculations. In-band structure calculations, We plotted the graph of energy versus the high symmetry k-points and then analyzed the properties of the substance on the basis of band lines and bandgap by using Gnuplot. To view the individual contribution of different orbital electrons, we study the conduction band edge and valance band edge.Similarly, the Density of states (DOS) is performed to get information about the nature of the bandgap and the Partial Density of states (PDOS) gives information about the origin of bands. In all these self-consistent fields (SCF) calculations, we have used the convergence criteria as the difference between energy in the order of 10^6 Rydberg.

In this chapter, we discuss about:

- Calculation of lattice parameter.
- Calculation of Density of states (DOS) as well as Partial Density of States (PDOS) and plotting.

Then we have performed the series of following convergence tests and energy minimization.

5.2 Structural Optimization:

We carried out the self- consistent field (scf) calculations to determine basic parameters: kinetic energy cut-off for the plane wave basis and k-points grid by testing the convergence of total energy with these parameters individually and calculation of lattice parameter by energy minimization.

5.2.1 Kinetic Energy cut-off (ecutwfc)

The plane wave scf code implemented in the Quantum Espresso expand the electron wave-function in terms of the infinite basis function that are plane waves. The value of the kinetic energy cut-off corresponds to the neighbouring interactions in the periodic system. If we take this cut-off energy large, we include long range interactions and the results will be more accurate, but this takes more computing resources. If we take this energy small, the results could be inaccurate though computationally cheap. Therefore, we have to take optimum value of this cut-off energy. It is expressed in unit of the energy Ry. The plane wave expansion in the reciprocal space is

$$\psi_k(r) = \frac{1}{\Omega}\sum_G \quad C_{k.G}e^{i(k+G).r} \tag{4.1}$$

where Ω is the volume of the box, G are the reciprocal lattice vectors defined by $G.l = 2\pi m$

for all l, where l is a lattice vector of the crystal and m is an integer, $C_{k.G}$ are the coefficients for the plane waves and k represent the reciprocal space vectors within the first Brillouin zone of the periodic cell.

In principle, we need infinite numbers of plane waves but in order to reduce the computational cost we have to truncate the plane wave expansion from some acceptable value. To make the plane wave expansion (4.1) finite, we truncated according to the condition.

$$\frac{|k+G|^2}{2m} \leq E_{cut} \tag{4.2}$$

We performed the scf calculations using the experimental value of the lattice parameter (a=8.2870 au,c=21.6358 au) and some arbitrary k-point mesh in the scf input file for Sb. The scf calculations were performed for different values of the ecutwfc ranging from 30 Ry to 100 Ry. At these different values of cut-off energy, we found different values of total scf energy. Then we plot the graph between the scf total energy versus kinetic energy cut-off value and the appropriate value of kinetic energy cut-off is chosen from which the convergence of total energy

starts to occur. In the case of Antimony, it is found to be 80 Ry, which is shown in the Fig. (4.1). So, for further calculations, the value of ecutwfc = 80 Ry is appropriate to use for Antimony. In our case, the pseudopotential used is PredewBerke-Erzndof (PBE) pseud o-potentials generated using "atomic" code by A. Dal Corso (espresso distribution). When a graph was plotted for the relationship between cut-off energy along X-axis versus total energy along Y-axis of Sb, following graph was obtained.

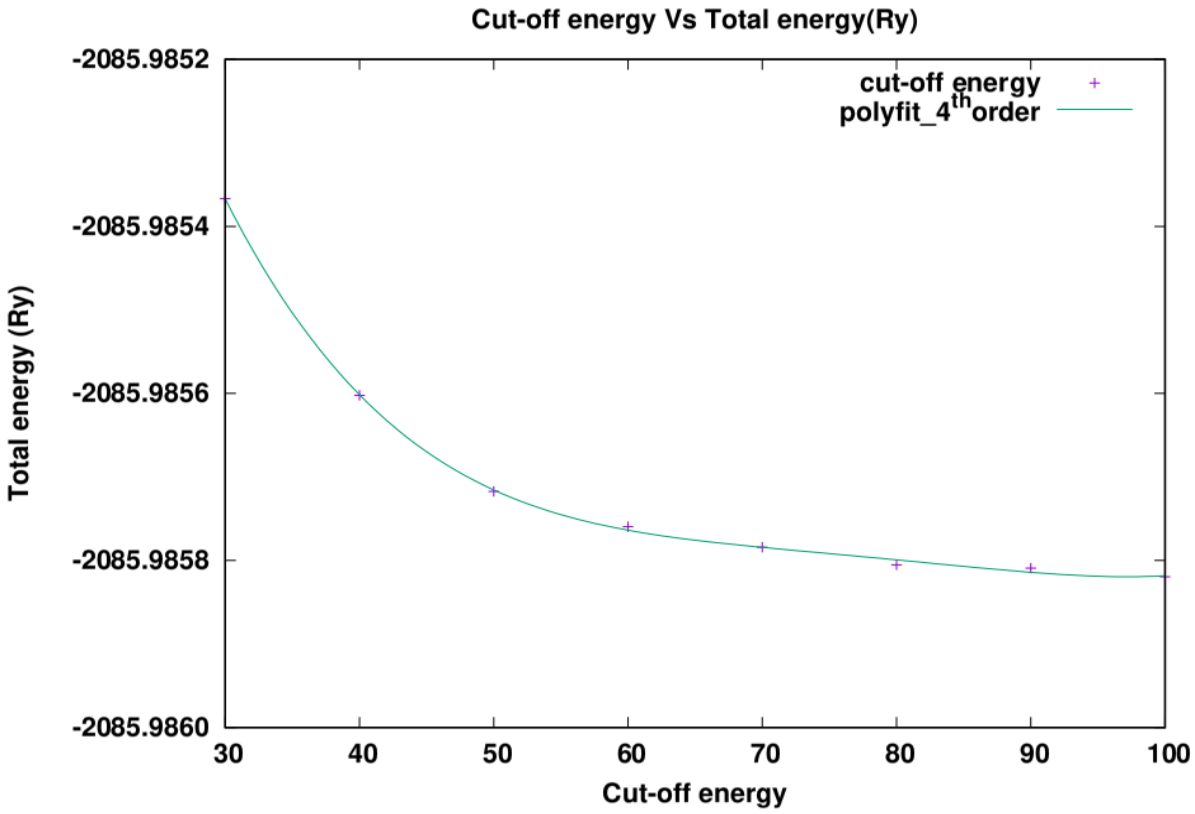

Figure 4.1: The plot of Total energy with cut-off energy of Sb

To determine the value of kinetic energy cut-off we performed the scf calculation using lattice parameter a=4.7459001541 angstrom from literature and some arbitrary k-point mess (10 10 10) in scf input file for Bismuth(Bi). Similarly, we perform same ecutwfc range as Bi in this case and we get different values of total energy in self-consistent field. Then plot of total energy versus kinetic energy cut-off value for base centered monoclinic structure of Bi is shown in Figure

(4.2). Clear from the Fig. (4.2) that there is nominal variation in total energy above 65 Ry. Therefore in the rest of calculations, our cut-off energy is 65 Ry.

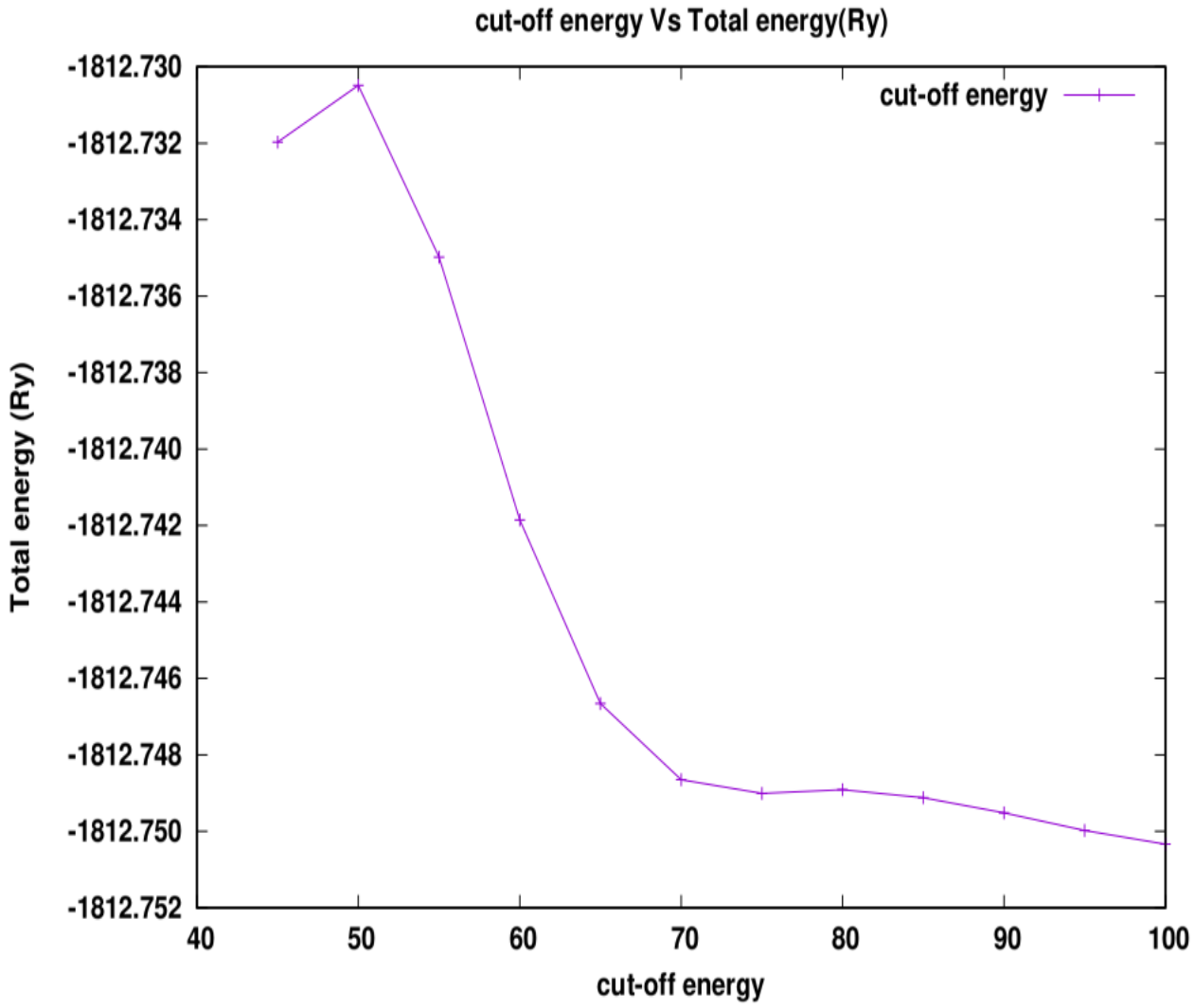

Figure 4.2: The plot of Total energy with cut-off energy of Bi

5.2.2 Lattice Parameter

Lattice constant is a property of crystal lattice that means periodic arrangement of atoms in three dimensions whether it is not a property of atoms. Basically, the lattice constant is the length of periodicity of the lattice repeats itself, for most crystals the lattice constant are few angstroms. After the calculation and value of ecutwfc and, we performed a convergence test for lattice

parameter by using the converged value of ecutwfc for both Sb and Bi. For Sb, we performed the scf calculations for total scf energy with different value of lattice parameters ranging from 7.7870 to 8.7870 Bohrs to optimizing lattice parameter by using optimized value of ecutwfc. Then we plot a graph between total energy with lattice parameter which is shown in Fig. 4.3

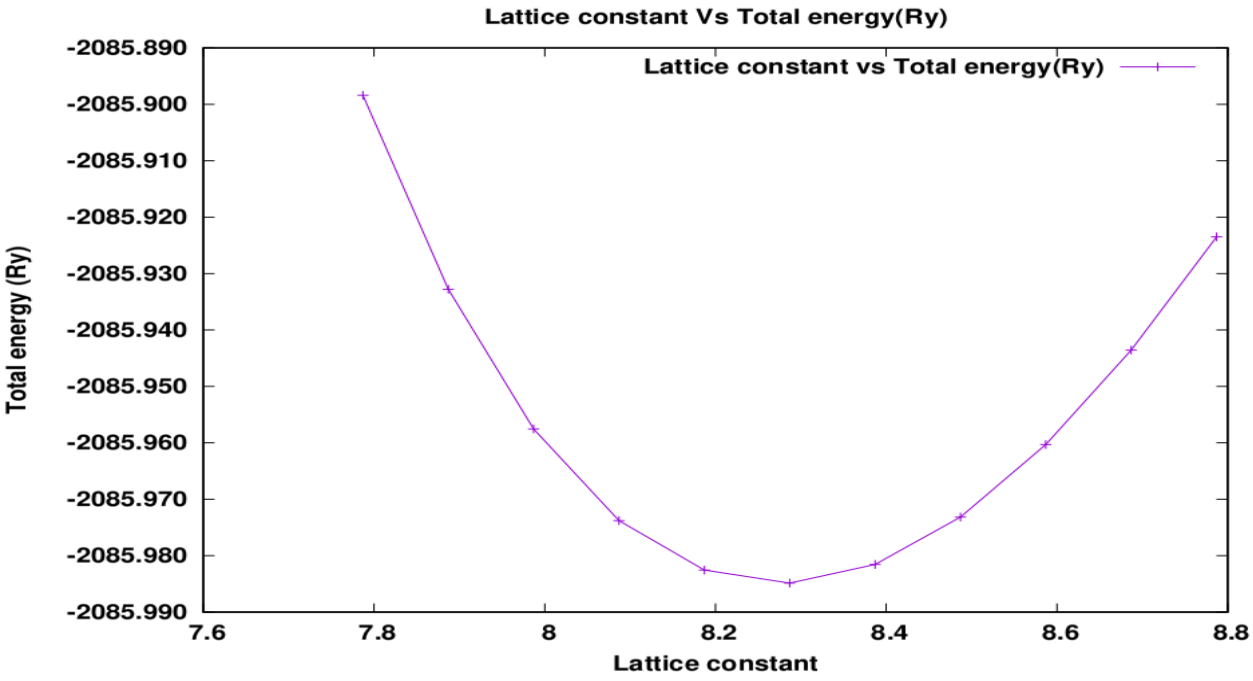

Figure 4.3: The plot of Total energy with lattice parameter of Sb

At different value of lattice parameter we found different value of total energy. Then, we obtained the suitable value of parameters for the input file at which the total energy is minimum. From Fig. 4.3, the appropriate value of lattice parameter is at which the minimum total energy is at 8.2870 Bohr. The experimental value of lattice parameter of Sb is very closer to our calculate value of lattice parameter.

To determine c/a ratio of Sb element structure ,we perform scf calculation by using optimized ecutwfc and lattice parameter.The scf calculation were performed in different value of the c/a ratio from 2.5608 to 2.6608 Bohr for Sb using pw.x . At different value of c/a we get different

value of total energy self-consistent field. Then we plot of total energy versus c/a ratio for Sb element which is shown in fig 4.4. From the figure, we found that the total energy is increases with increase the c/a ratio and get minimum value at 2.6108 Bohr which is our optimized value of Sb.

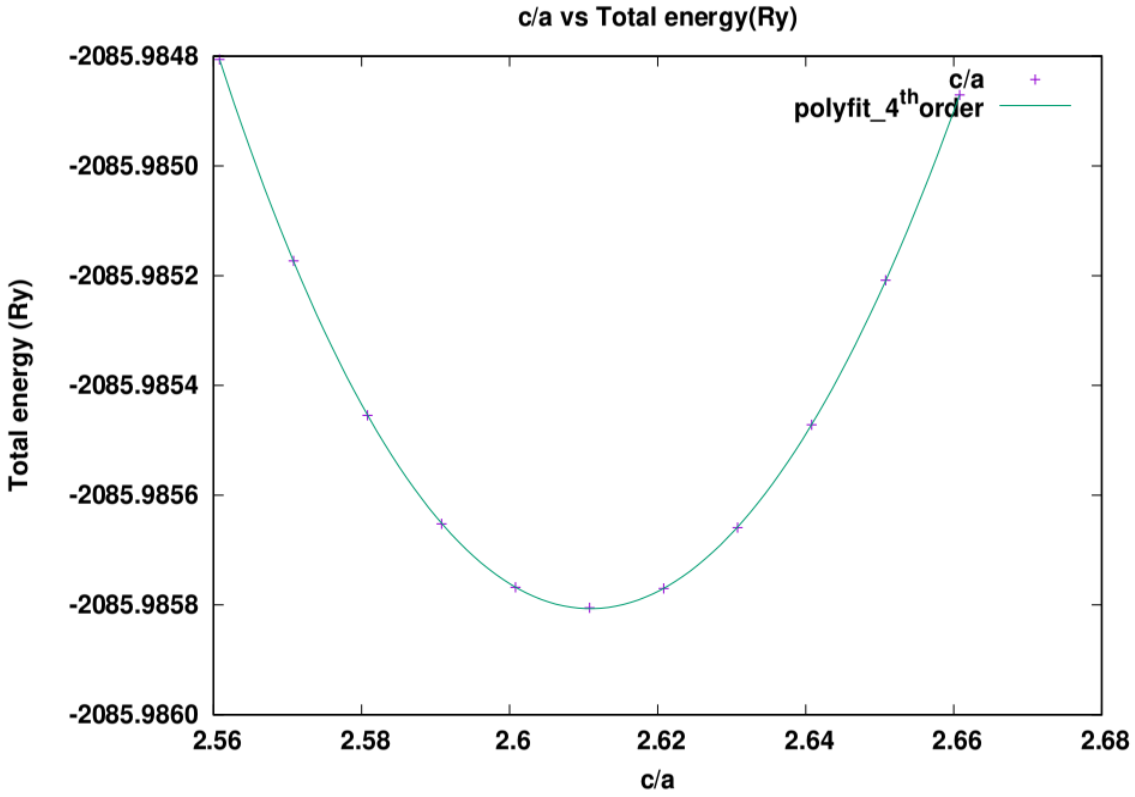

Figure4.4: The plot of Total energy with c/a ratio of Sb

Similarly, For Bi we performed the scf calculations for total scf energy with different value of lattice parameters ranging from 4.1459001541 to 5.2459001541 Bohr by using optimized ecutwfc. we obtained the suitable value of parameters for the input file for Bi at which the total energy is minimum. From Fig. 4.5, the minimum total energy is at 4.7459001541 Bohr. The experimental value of lattice parameter is found closer to our calculate value of lattice parameter.

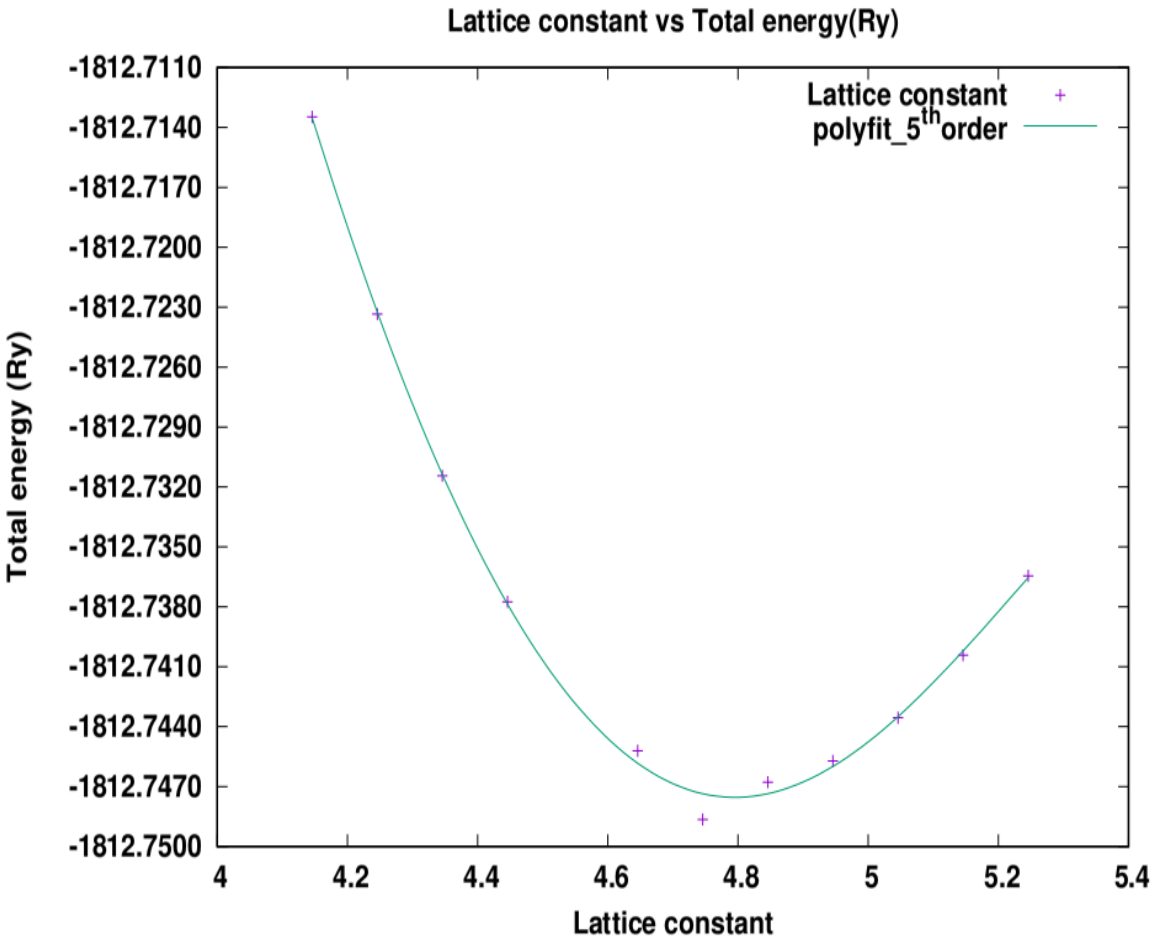

Figure 4.5: The plot of Total energy with lattice parameter of Bi

5.2.3 k-point grid

In order to perform the Brillouin zone interaction in discrete scheme, it is essential to have a large number of grid points.Due to limitations of computational resources, we optimize the number of k-points grids. By calculating total energy versus k-point grids the rectangular grid of points of dimensions Kx×Ky×Kz spaced evenly throughout the Brillouin zone is called k-points grid. More the number of the grid points sampling will be more finer and accurate but computationally expensive. Here, the size of grid required depends on the system under study. We can estimate appropriate size by means of total energy calculation. Our approach of k-point sampling is as suggested by Monkhrost and Pack **[37]**.

At first, we performed the scf calculations of Sb for total scf energy with different values of k-points grid starting from 2×2×2 to 10×10×10. The calculated data of k-point grid vs its corresponding total scf energy is shown in Fig. 4.6.

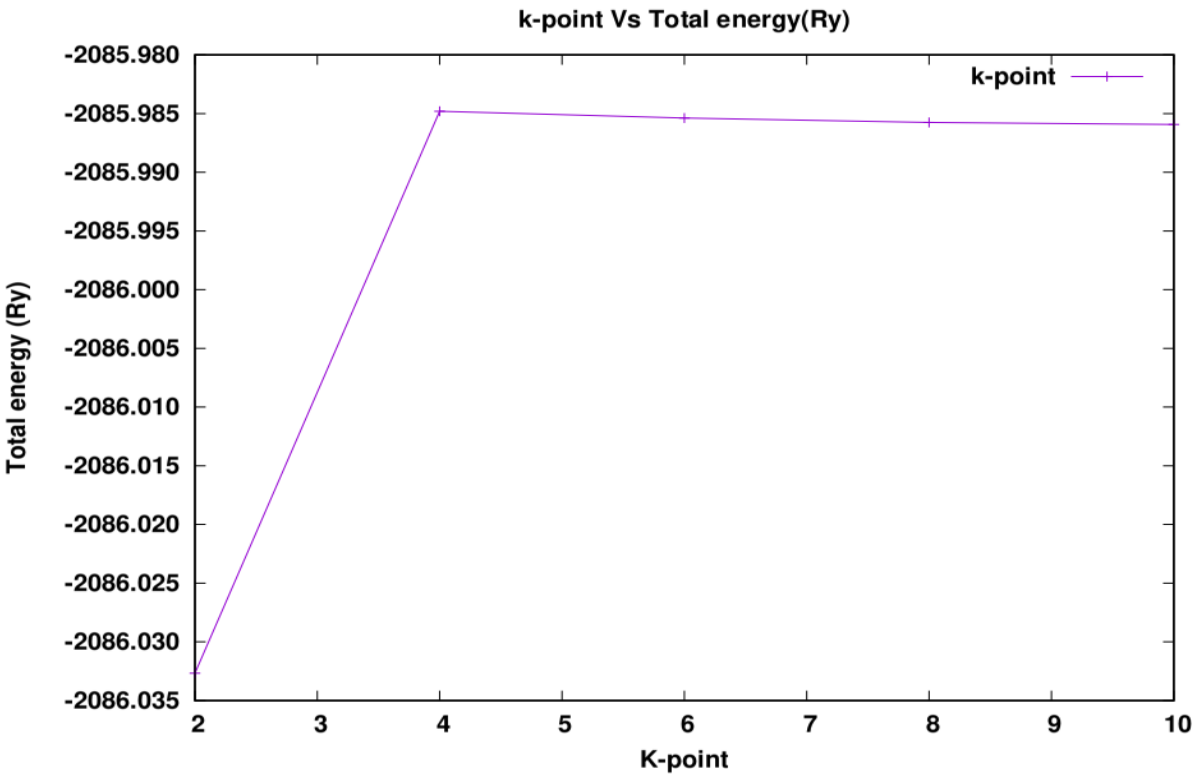

Figure4.6: The plot of Total energy with k-point grid of Sb

From Fig. 4.7, is clearly seen that total energy of Sb remains almost constant from the k-point grid 8×8×8 So, it is appropriate to use the value of k-point grid as 8×8×8 for our further calculation. Then we performed the scf calculations of Bi for total scf energy with different values of k-points grid starting from 2×2×2 to 16×16×16. The calculated data of k-point grid vs its corresponding total scf energy is shown in Fig. 4.7.

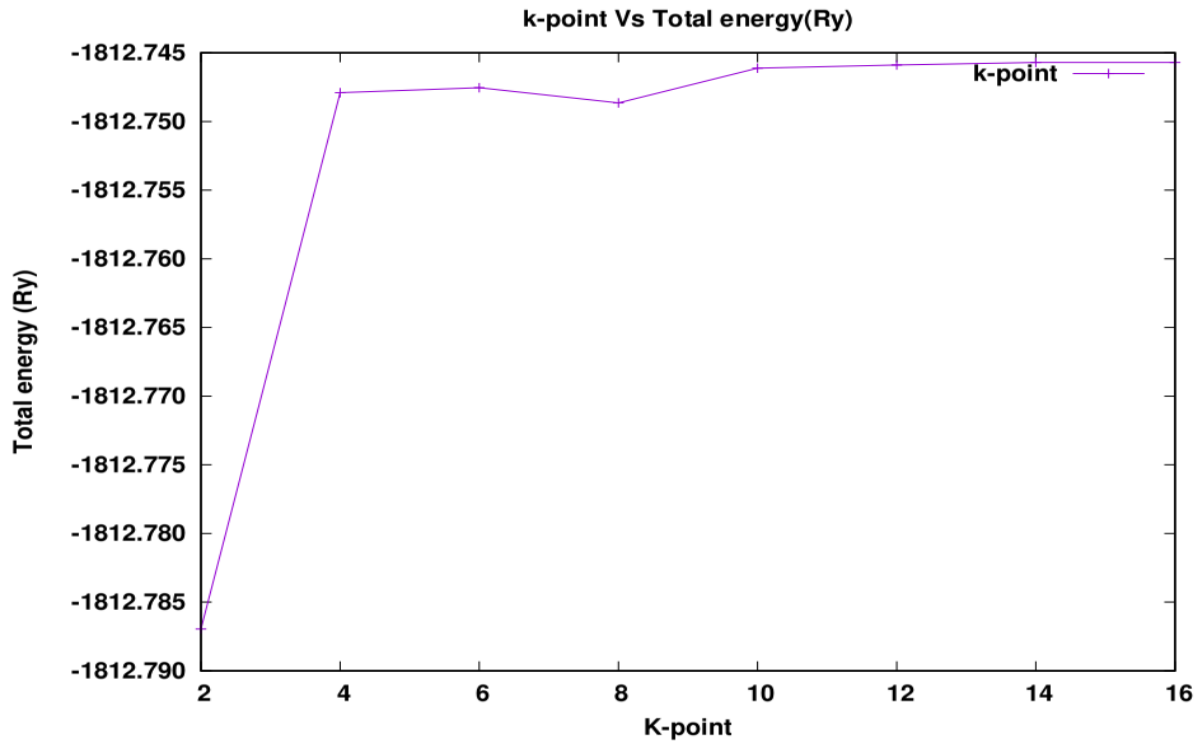

Figure4.7: The plot Total energy with k-point grid of Bi

From Fig. 4.7, it is clearly seen that total energy remains almost constant from the k-point grid10×10 ×10 So, it is appropriate to use the value of k-point grid as 10×10 ×10 for our further calculation.

5.2.4 Degauss

In the case of degauss, you should use the smallest value at which your calculation does not struggle to converge. After optimization of all Structure of Sb and Bi we are intended to study the effect of degauss on elements. To account the degauss, we have taken all optimized value and apply degauss in the range of 0.001 to 0.01. Then we plotted a graph between degauss value vs total kinetic energy which is shown in Figure 4.8 and figure 4.9 for Sb and Bi respectively. From the graph it is observed that degauss is constant to 0.001 for Sb so further calculation take place by using degauss 0.001 and for Bi degauss is observed as 0.01 for further calculations.

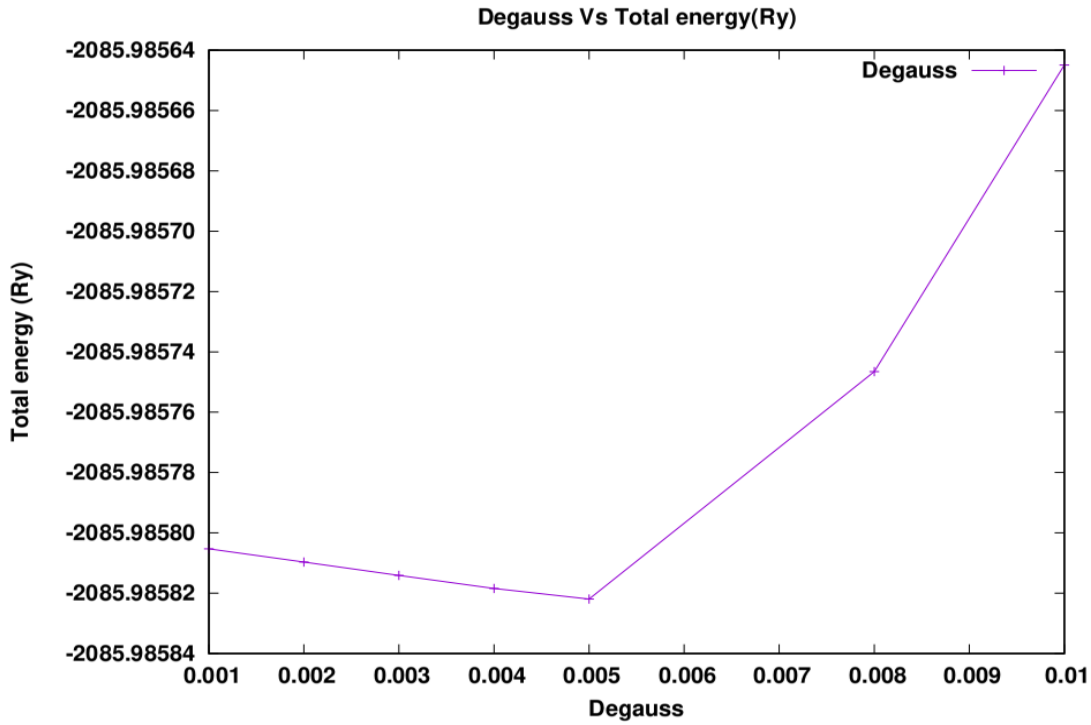

Figure 4.8: The plot of Total energy with degauss of Sb

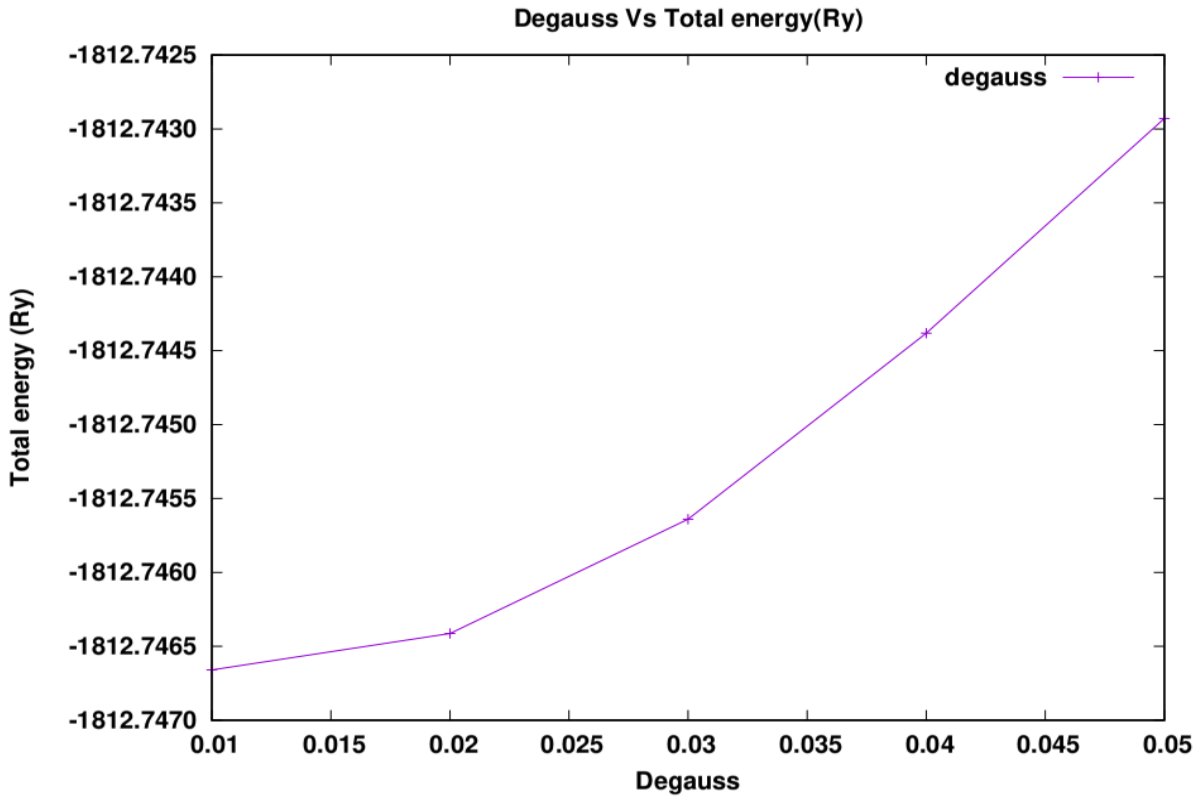

Figure 4.9: The plot of Total energy with degauss of Bi

We have also calculated the band structure of Sb and Bi. For other calculations of Sb and Bi , we took (8×8×8) and(10×10 ×10)respectively k-points along specific direction of irreducible Brillouin zone in order to obtain fine band structure which is performed by executable pw.x. Then, we performed post processing calculations with executable plotband.x in order to obtain band structure of Antimony and Bismuth.Further, we have calculated the DOS and PDOS for both Sb and Bi structure. Finally we performed scf calculation and then nscf calculation; we used denser k-point mesh in order to obtain smooth partial density of states curve. These calculations were performed using the executable pw.x. Then, we performed PDOS calculation using executables projwfc.x command. In this section, we discussed the results of the first principles calculations carried out to obtain: Band structure calculation of Sb and Bi, Density of states of structure and Partial Density of states of structure of Sb and Bi.

5.3 Band Structure

In the first principles electronic structure calculation of crystals, the electronic band structure is one of the most widely applied analytical tools especially within the Kohnsham framework of density functional theory. The band structures of solid are helpful to determine different electronic properties of solid. It contains the basic ingredients to almost all the crystal properties. Since the atoms in a solid are closely packed the interaction between them perturbed the initial atomic levels when a large number of atoms are brought together. Electrons in the orbitals are filled up according to Pauli's exclusion principle i.e. no two electrons can occupy the same energy state. A bands constitutes a sort of energy continuum, in which separate level due to individual atoms cannot be identified. In the process of inter atomic interaction, the inner shell electron stated are the least affected. Whereas the valance electron, which are closest to neighbouring ions, are the most affected. The effect of bringing one atom closer to the other is to split a single sharp level. The bands structures of solids are helpful in determining different electronic and optical properties of the solid.The band structure is calculated by pseudo potential

and plane wave basis set method within the Density functional theory (DFT), treating exchange-correlation functional with generalized gradient approximation (GGA) in the form of PredewBerke- Erzndof (PBE) functional. All pseudo potential used in the calculations were norm- conserving scalar relativistic and full relativistic pseudo potentials. All calculation was performed within the Quantum- ESPRESSO package, plane wave kinetic energy cut-off were set at 80 Ry for Sb and 65 Ry for Bi. We took uniform grid of k-vector (k-points) in X-Y plane ranging from 1 to 1 in the unit of 2π a .

The band structure calculation of Sb obtained is shown in Fig. 4.10.From graph,the calculated value of band gap is found to be nearly 0ev because of the overlap at M (k-paths).Our work result is nearly same as previous calculated work.**[17]**

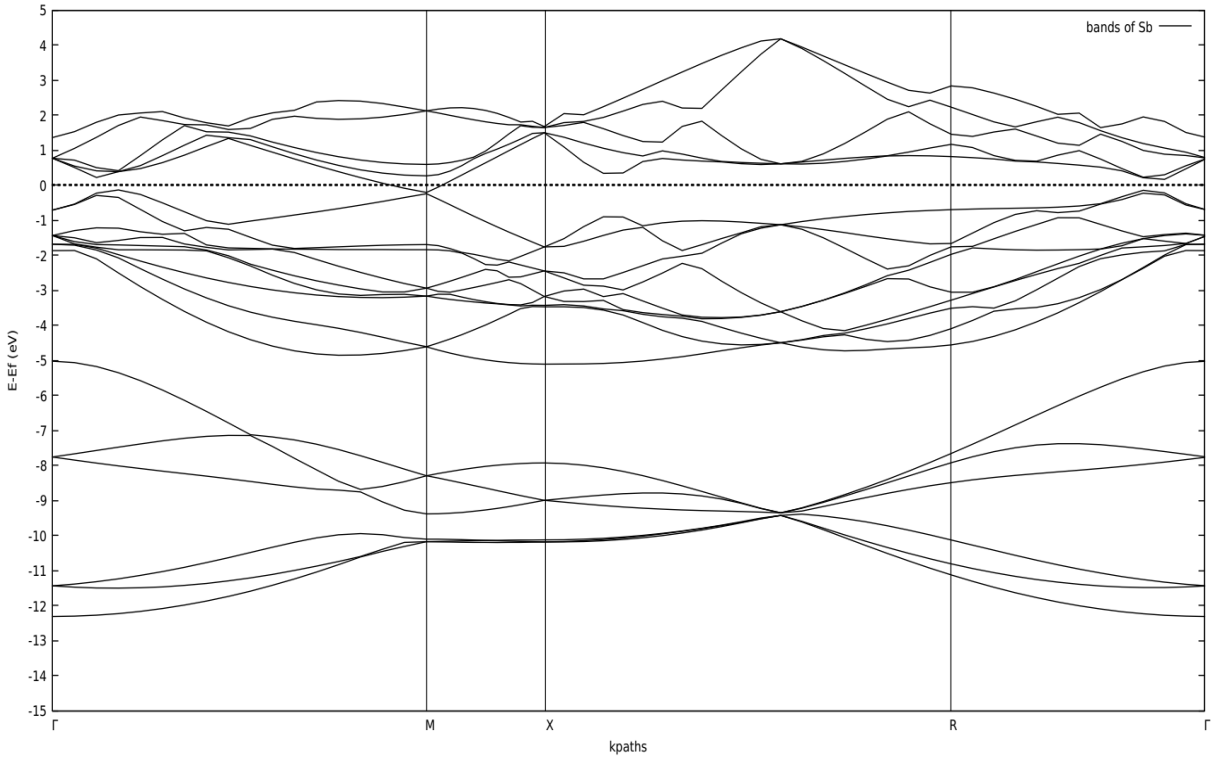

Figure4.10: the plot of energy gap between conduction and valence band of Sb

The band structure calculation of Bi is shown in Fig. 4.11.From graph,the calculated value of band gap is found to be nearly 0ev because of the overlap at R (k-paths).Our work result is nearly same as previous calculated work.**[13]**

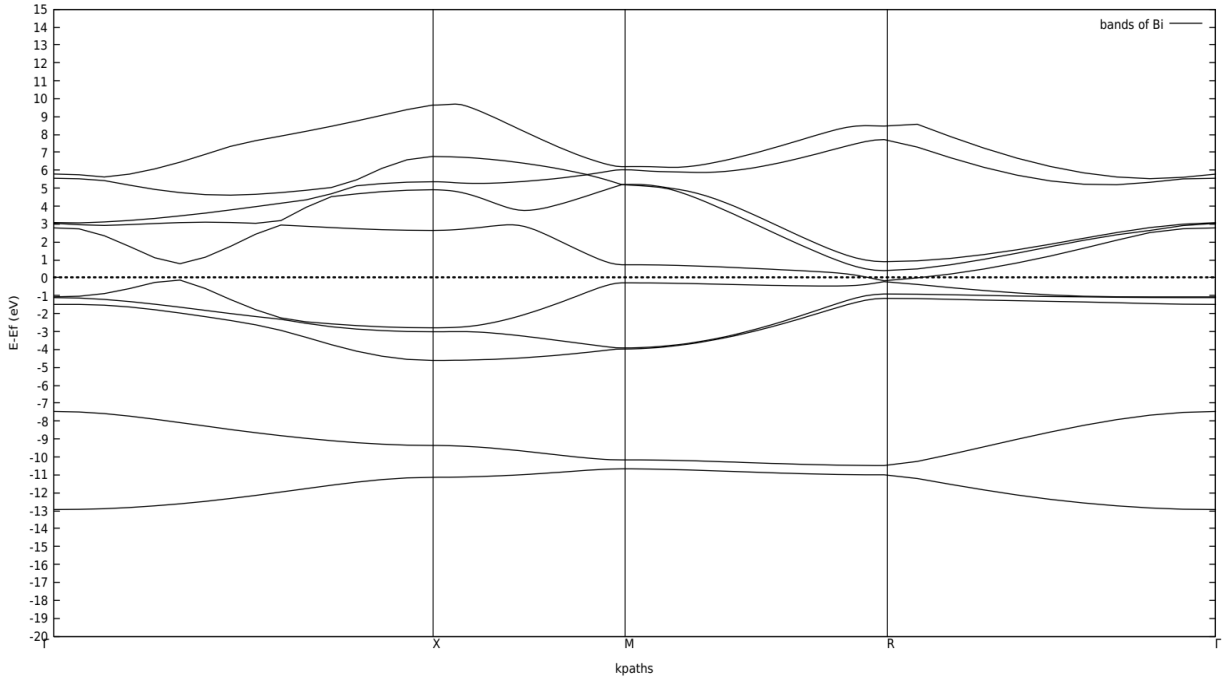

Figure 4.11: The plot of energy gap between conduction and valence band of Bi

5.4 Density of States

The density of states (DOS) is defined as the number of states per unit energy range available for the particles to be occupied. In other words, the density of states refers to the number of quantum states per unit energy range and it indicates how density packed quantum states in a particular system. In solid state and condense matter physics, the density of states is of immense important as it can be used to calculate the various parameters that give the insight of the different electronic, magnetic and transport properties. For example, Specific heat and paramagnetic susceptibility of a substance, mobility of charge carriers, diffusion properties and so on can be readily computed with the knowledges of density of states (DOS). Moreover, the density of states provides numerical information on the states that are available at each energy level. The value of zero density of states indicates that there are no available states for occupation in an energetic level

The density of sates is calculated by pseudopotential and plane wave basis set method within the Density functional theory (DFT), treating exchange- correlation functional with generalized gradient approximation (GGA) in the form of PredewBerke- Erzndof (PBE) functional. All pseudopotential used in the calculations were norm- conserving scalar relativistic and full relativistic pseudopotentials. All calculation was performed within the Quantum- ESPRESSO package, plane wave kinetic energy cut-off was set at 80 Ry for Sb and 65 Ry for Bi.

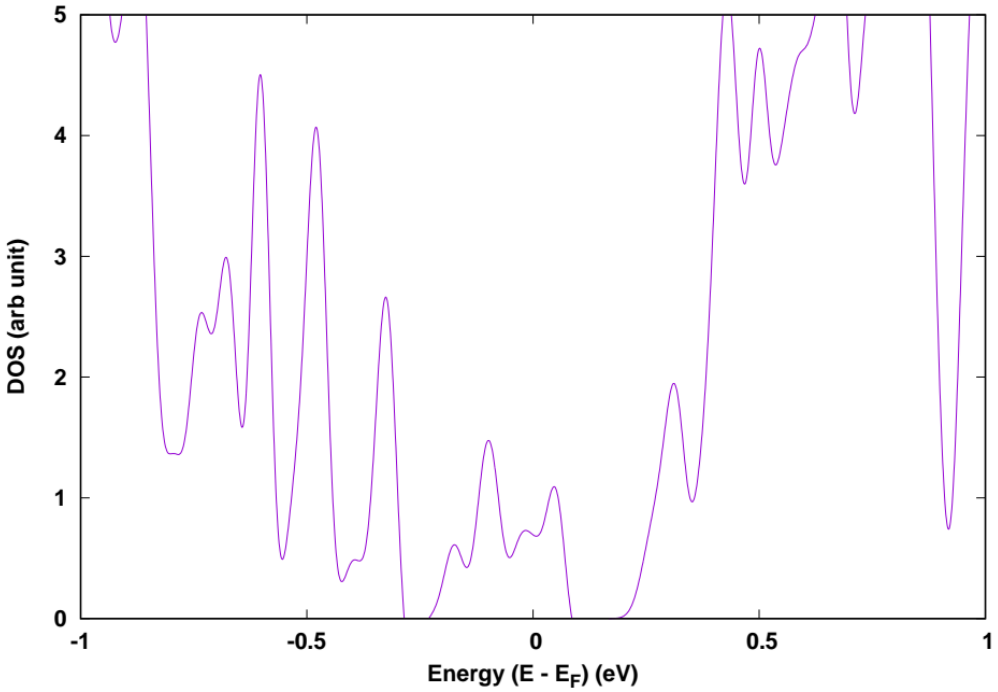

Figure4.12: DOS curve of Sb with energies at DeltE=0.01

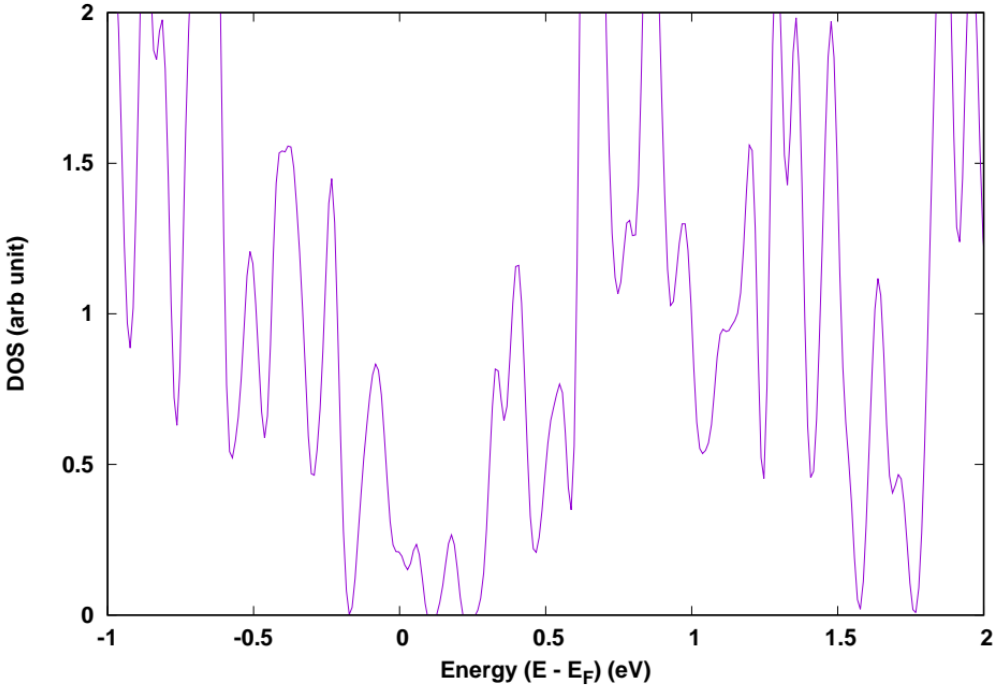

Figure4.13: DOS curve of Bi with energies at DeltE=0.01

The results of density of Sb and Bi help to further elaborate the nature of the band gap as shown in above Fig. 4.12 and Fig. 4.13, Where density of states DeltE=0.01, shows the respective states of crystal which clarify the nature of the element. The band gap of Sb and Bi is found to be 0.15 ev and 0.09 ev respectively which is quite similar to referance value.For the comparative study of the band structures and density of states, we have merge the figure of band structures and density of states of Sb and Bi in suitable scale which is shown in Fig.4.14 and Fig.4.15 respectively.

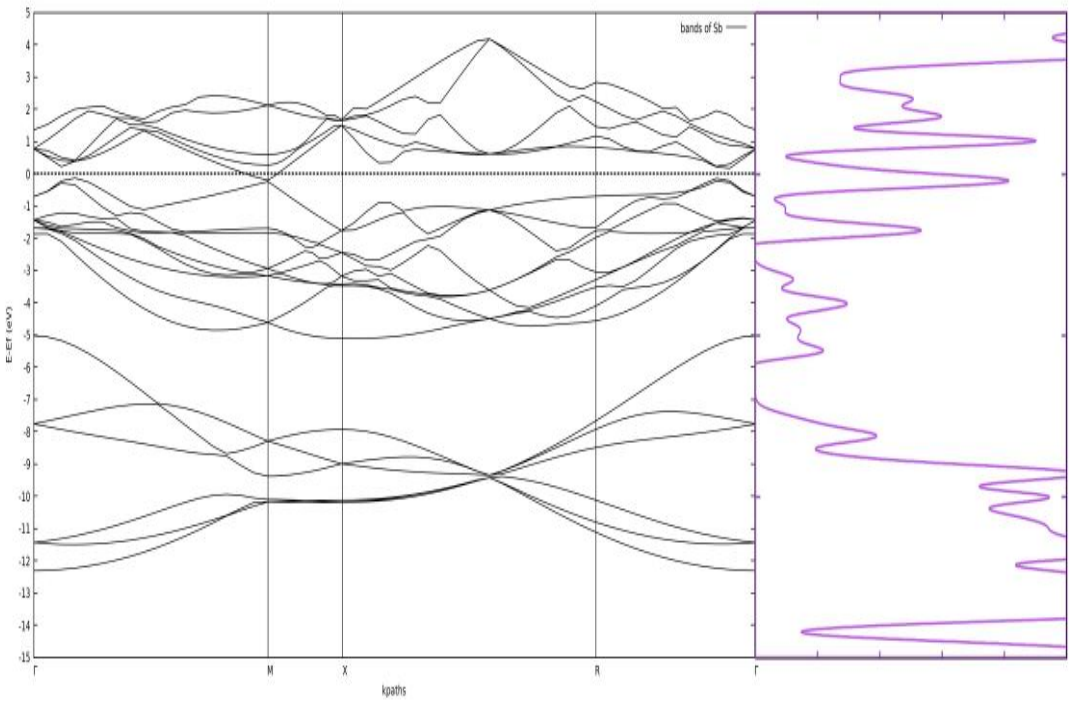

Figure4.14: comparative study of the band structures and density of states of Sb

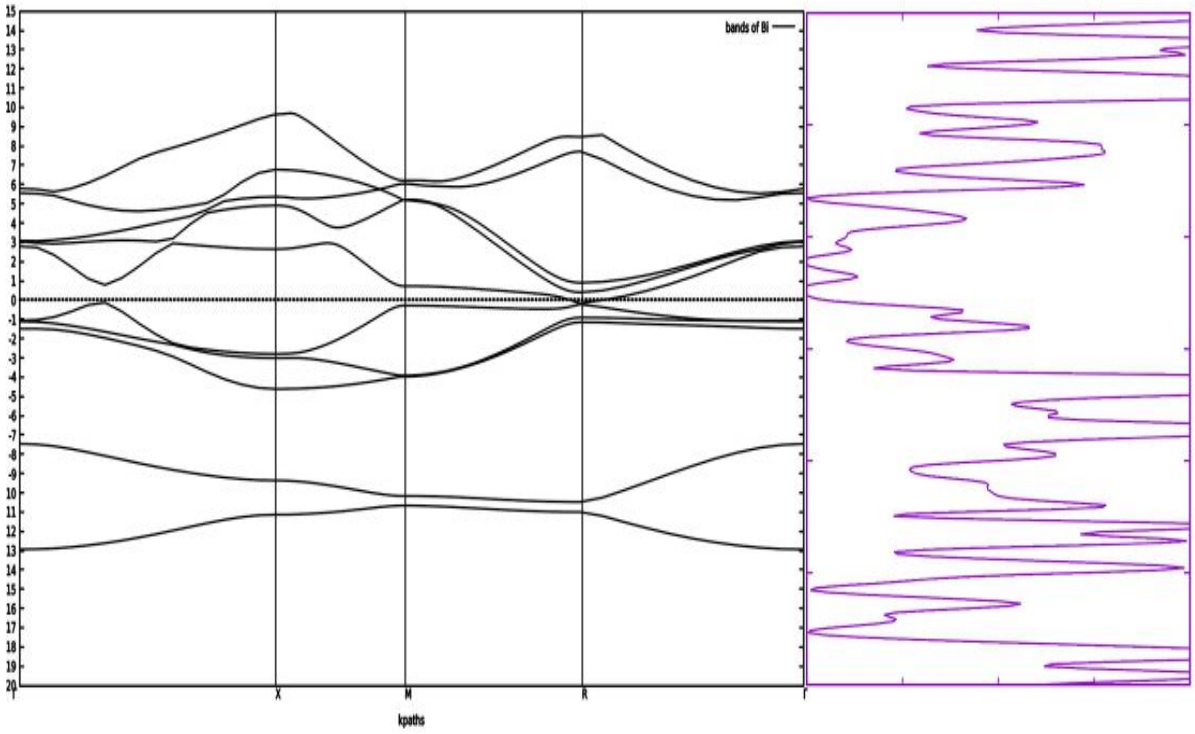

Figure4.15: comparative study of the band structures and density of states of Bi

CHAPTER 6

CONCLUSION AND CONCLUDING REMARKS

This thesis has successfully employed to examine the structural properties of group 15 semimetals Sb and Bi with the help of DFT, GGA, implemented with Quantum ESPRESSO code. At first we have constructed optimized structure of unit cell structure of both Sb and Bi. During optimization, the kinetic energy cut-off energy is found to be 80 Ry having k-point grid $8 \times 8 \times 8$ for Sb. Then we estimate the lattice Parameter is found to be 8.2870 au for Sb which is very near with experimental results as well as previous calculated data.Thus the lattice parameter of Sb estimated with GGA method is in close agreement with experimental values. Then we have study the band structure, density of states and partial density of states of Sb using GGA method in QE package.

Similarly, optimization, the kinetic energy cut-off energy is found to be 65 Ry having k-point grid $10 \times 10 \times 10$ for Bi. Then we estimate the lattice Parameter is found to be 4.7459001541 Bohr for Bi which is very near with experimental results as well as previous calculated data.Thus the lattice parameter of Bi estimated with GGA method is in close agreement with experimental values. Then we have study the band structure, density of states and partial density of states of Bi using GGA method in QE package.

This shows that Quantum ESPRESSO code using the plane-wave pseudopotential method can be used to perform first-principles calculations to study the electronic and other system which is more complex for heavier elements of group 15. We belive code can be used to study correlated systems for interest to current research to amble technological potential they support. All our study method which we have performs in this work can be used standard frame work to calculate the electronic, magnetic, and structural properties of materials in the elements and other related materials for which experimental data are not available.

6.1 Further Enhancement

The following studies can be done as further enhancement in our present study.

- Similar study from semimetal at least few more candidates, possibly adding optical,magnetic and phonon properties can be done in future.
- We also can study the effect of doping of other suitable atom, which would give rise to alloy of different properties and can applicable for further research.
- We also can study same properties by using other different methods suitable for these elements.

And finally we are now still willing to extend our work to study the magnetic properties and phonon calculation, thermal expansion, optical properties which may have many potential applications in modern electronics.

BIBLIOGRAPHY

[1] Solid state physics, R.Murugeshan, Kiru Thiga and Siva Prashad, *8th Edition (2001)*

[2] Robert H. Crabtree, *The Organometallic Chemistry of the Transition Metals* John Wiley & Sons, Inc., Hoboken, New Jersey (2014)

[3] J. R. Hook, H. E. Hall, *Solid state physics*, Wiley (1991)

[4] Harald Ibach, Hans L., *Solid-state physics an introduction to Principle of material science*, Springer Verlag Berlin Heidelberg, (2009)

[5] Richard J. D. Tilley - *Crystals and Crystal Structures*, Wiley (2006)

[6] Giuseppe Iadonisi, Giovanni Cantele, Maria Luisa Chiofalo, *Introduction to Solid State Physics and Crystalline Nanostructures*, Springer-Verlag Mailand, (2014)

[7] Charles Kittel *Introduction to Solid State Physics*, Wiley (2005)

[8]J W Mullin *Crystallization*, Butterworth-Heinemann (2001)

[9] *Solid State Physics-Ashcroft,Neil W,Mermin,David N*

[10] https://education.jlab.org (Retrived 15 may 2020)

[11] Vishnu Swarup Mathur, Surendra Singh - *Concepts in Quantum Mechanics*-Chapman &Hall_CRC (2009)

[12] F. Bloch, Uber die Quantenmechanik der Electronen in kristallgittern, Zeits., F. Physik , 52, 555-600, (1928).

[13] Introduction to Modern Solid State Physics Yuri M. Galperin FYS 448,pg 56,57

[14] https://rsc.org/periodic-table/element/antimony and bismuth (Retrived 19 may 2020)

[15] Advances in Physics 1976 , vol.25, no. 6,555 - 613 V.s.Edel'Man

[16] First principles study of As,Sb,Bi 1990Gonze, Xavier ; Michenaud, Jean-Pierre ; Vigneron, Jean-Pol

[17] Phy.Review B Yi Liu and Roland E. Allen Vol.52 15 july 1995-I

[18] [First principles study of As,Sb,Bi 1990Gonze, Xavier ; Michenaud, Jean-Pierre ; Vigneron, Jean-Pol

[19] Ph. Hofmann / Progress in Surface Science 81 (2006) 191–245

[20] IBM J.Res. Develop.8,215(1964)

[21] L.M.Falicov and S.Golin,phys.Rev.137,A871(1965)

[22] X.Gonze and J.P.Michenaud,phys review B,Vol.14,Number 17,15th june,1990

[23] J.P. Issi,Aust.J.phys.32,585(1979)

[24] A. Ogg (1922) Crystalline structure of Antimony and Bismuth transactions of the Royal Society of South Africa, 75-80

[25] Physical review by L.M. Falicov and P.J. Lin,Volume41 no.2,Jan.1966

[26] S.Mase,J.phys.soc.Jpn.13,434(1958);14,584 (1959)

[27] D.Weaire and A.R. williams ,physics of semi-metals and narrow gap semiconductors

[28] EfthimiosKaxiras - *Atomic and electronic structure of solids*, Cambridge University Press (2003)

[29] David S. Sholl, Janice A. Steckel - *Density Functional Theory A Practical Introduction*, Wiley (2009)

[30] Philip L. Taylor, OlleHeinonen, *A quantum approach to condensed matter physics* Cambridge University Press, (2002

[31] V. Antonov, B. Harmon, A. Yaresko *Electronic Structure and Magneto-Optical Properties of Solids*, Kluwer Academic Publishers, (2004)

[32] Richard M. Martin, *electronic structure basic theory and practical methods*, Cambridge University press (2004)

[33] Mark Fox, *Optical properties of solids*, Oxford University Press (2001)

[34] David A. B.Miller, Quantum Mechanics for Scientistsand Engineers, Cambridge University Press (2008)

[35] Victor Antonov,Bruce Harmon, Alexander Yaresko, *Electronic Structure and Magneto-Optical Properties Of Solids*, Kluwer Academic Publishers New York, Boston, Dordrecht, London, Moscow (2004)

[36] https://nanohub.org/resources/27109 (Retrived 2 June 2020)

[36] P. Giannozzi *Hands-on Tutorial on Electronic Structure Computations* (2013)

[37] Algorithm PWscf User's Guide (v.6.5MaX)

[38] Brian G. Moore School of Science, Penn State Erie–The Behrend College, Erie, PA 16563-0203;bgm4@psu.edu

APPENDIX

[A]. LIST OF TABLES:

Table 1: Table of cut-off kinetic energy and its corresponding total energy of Sb:

cut-off energy (Ry)	Total energy (Ry)
30	-2085.98536685
40	-2085.98560235
50	-2085.98571737
60	-2085.98575969
70	-2085.98578409
80	-2085.98580530
90	-2085.98580919
100	-2085.98581960

Table 2: Table of cut-off kinetic energy and its corresponding total energy of Bi

cut-off energy (Ry)	Total energy (Ry)
45	-1812.73196780
50	-1812.73048964
55	-1812.73497745
60	-1812.74185423
65	-1812.74665889
70	-1812.74864952
75	-1812.74900565
80	-1812.74891245
85	-1812.74912096
90	-1812.74951358
95	-1812.74997694
100	-1812.75033709

Table 3: The Variation of total energy with k-point grid of Sb

K-point	Total energy (Ry)
2	-2086.03267421
4	-2085.98481194
6	-2085.98537479
8	-2085.98575972
10	-2085.98592299

Table 4: The Variation of total energy with k-point grid of Bi:

K-point	Total energy (Ry)
2	-1812.78695703
4	-1812.74789944
6	-1812.74754483
8	-1812.74864952
10	-1812.74611750
12	-1812.74588227
14	-1812.74570532
16	-1812.74570481

Table 5: The Variation of total energy with lattice constant of Sb:

Lattice constant(Bohr)	Total energy (Ry)
7.7870	-2085.89840211
7.8870	-2085.93279407
7.9870	-2085.95753435
8.0870	-2085.97378346
8.1870	-2085.98255201
8.2870	-2085.98485852
8.3870	-2085.98154680
8.4870	-2085.97315045
8.5870	-2085.96030188
8.6870	-2085.94357226
8.7870	-2085.92347985

Table 6: The Variation of total energy with lattice constant of Bi:

Lattice constant (Bohr)	Total energy (Ry)
4.1459001541	-1812.71346451
4.2459001541	-1812.72334079
4.3459001541	-1812.73143757
4.4459001541	-1812.73775542
4.6459001541	-1812.74521495
4.7459001541	-1812.74864952
4.8459001541	-1812.74678314
4.9459001541	-1812.74572057
5.0459001541	-1812.74355691
5.1459001541	-1812.74042276
5.2459001541	-1812.73644956

Table 7: The Variation of total energy with lattice constant (c/a) of Sb:

Lattice constant (c/a)	Total energy (Ry)
2.5608	-2085.98480599
2.5708	-2085.98517290
2.5808	-2085.98545436
2.5908	-2085.98565205
2.6008	-2085.98576769
2.6108	-2085.98580530
2.6208	-2085.98576988
2.6308	-2085.98565904
2.6408	-2085.98547152
2.6508	-2085.98520827
2.6608	-2085.98487068

Table 8: The Variation of total energy with degauss of Sb:

Degauss	Total energy (Ry)
0.001	-2085.98580530
0.002	2085.98580966
0.003	-2085.98581411
0.004	-2085.98581843
0.005	-2085.98582192
0.008	-2085.98574655
0.010	-2085.98564493

Table 9: The Variation of total energy with degauss of Bi:

Degauss	Total energy (Ry)
0.01	-1812.74665889
0.02	-1812.74641296
0.03	-1812.74563979
0.04	-1812.74438127
0.05	-1812.74292947

[B]. Different input Files:

List 1: Input script for scf final

Sb

```
&CONTROL
   calculation    = "scf"
   restart_mode   ='from_scratch'
   prefix         ='Sb'
   pseudo_dir='/home/surya/espresso/pseudo'
   outdir='./'
!  disk_io= 'high'
!  tstress=.TRUE.
!  tprnfor=.TRUE.
/
&SYSTEM
   ibrav          = 4
   celldm(1)      = 8.2870 ! au
!  c              = 21.6358 ! au
   celldm(3)      = 2.6108
   ecutwfc        = 80
   ecutrho        = 800
```

```
   nat           = 6
   ntyp          = 1
   occupations    = 'smearing'
   smearing       = 'mv'
   degauss        =  0.001
/
&ELECTRONS
   conv_thr        =  1.0d-07
   electron_maxstep = 200
   mixing_beta      = 0.7
   startingpot      = 'atomic'
   startingwfc      = 'atomic+random'
/
ATOMIC_SPECIES
 Sb 121.76  Sb.pbe-n-kjpaw_psl.1.0.0.UPF
ATOMIC_POSITIONS {crystal}
  Sb  0.000000000        0.000000000        0.266833984
  Sb  0.000000000        0.000000000        0.733165974
  Sb  0.666666667        0.333333335        0.600167317
  Sb  0.666666667        0.333333335        0.066499354
```

Sb 0.333333325 0.666666669 0.933500609

Sb 0.333333325 0.666666669 0.399832683

K_POINTS {automatic}

8 8 7 1 1 1

Bi

&control

calculation='scf'

restart_mode='from_scratch',

prefix='Bi'

pseudo_dir = /home/surya/espresso/pseudo',

outdir='./'

tstress=.TRUE.

tprnfor=.TRUE.

/

&system

ibrav = 0

nat = 2,

ntyp = 1,

occupations = 'smearing',

smearing = 'mv',

```
   degauss = 0.01,
   ecutwfc = 65.0
   ecutrho = 260.0
/
&electrons
   mixing_beta=0.7
   conv_thr =  1.0d-08
/
CELL_PARAMETERS {angstrom}
  4.7459001541        0.0000000000        0.0000000000
  2.5683164347        3.9909045296        0.0000000000
  2.5683164347        1.4013675379        3.7367750786
ATOMIC_SPECIES
  Bi  208.98038  Bi.pbe-dn-kjpaw_psl.1.0.0.UPF
ATOMIC_POSITIONS {crystal}
  Bi   0.237000021        0.237000010        0.237000003
  Bi   0.763000115        0.762999983        0.763000050
K_POINTS AUTOMATIC
 10 10 10 1 1 1
```

List 2: Input script for nscf

Sb

```
&control
    calculation='nscf'
    restart_mode='from_scratch',
    prefix='Sb'
    pseudo_dir='/home/surya/espresso/pseudo'
    outdir='./'
!    disk_io= 'high'
!    tstress=.TRUE.
!    tprnfor=.TRUE.
/
&SYSTEM
    ibrav          = 4
    celldm(1)      = 8.2870 ! au
 !   c              = 21.6358 ! au
    celldm(3)      = 2.6108
    ecutwfc        = 80
    ecutrho        = 800
    nat            = 6
```

```
   ntyp           = 1
   nbnd           = 20
   occupations    = 'smearing'
   smearing       = 'mv',
   degauss        =  0.001
/
&ELECTRONS
   conv_thr        =  1.0d-07
   electron_maxstep = 200
   mixing_beta      = 0.7
   startingpot      = 'atomic'
   startingwfc      = 'atomic+random'
/
ATOMIC_SPECIES
  Sb 121.76  Sb.pbe-n-kjpaw_psl.1.0.0.UPF

ATOMIC_POSITIONS {crystal}
  Sb  0.000000000        0.000000000        0.266833984
  Sb  0.000000000        0.000000000        0.733165974
  Sb  0.666666667        0.333333335        0.600167317
```

```
 Sb  0.666666667        0.333333335        0.066499354
 Sb  0.333333325        0.666666669        0.933500609
 Sb  0.333333325        0.666666669        0.399832683
K_POINTS {automatic}
 8 8 7  0 0 0
```

Bi

```
&control
    calculation='nscf'
    restart_mode='from_scratch',
    prefix='Bi'
    pseudo_dir='/home/surya/espresso/pseudo'
    outdir='./'
!    disk_io= 'high'
!    tstress=.TRUE.
!    tprnfor=.TRUE.
/
&system
    ibrav = 0
    nat = 2,
    ntyp = 1,
```

```
   nbnd = 20,
   occupations = 'smearing',
   smearing = 'mv',
   degauss = 0.01,
   ecutwfc = 65.0
   ecutrho = 260.0
/
&electrons
   mixing_beta=0.7
   conv_thr =  1.0d-08
/
CELL_PARAMETERS {angstrom}
  4.7459001541        0.0000000000        0.0000000000
  2.5683164347        3.9909045296        0.0000000000
  2.5683164347        1.4013675379        3.7367750786
ATOMIC_SPECIES
  Bi  208.98038  Bi.pbe-dn-kjpaw_psl.1.0.0.UPF
ATOMIC_POSITIONS {crystal}
  Bi   0.237000021        0.237000010        0.237000003
  Bi   0.763000115        0.762999983        0.763000050
```

```
K_POINTS AUTOMATIC
  10 10 10 0 0 0
```

List 3: Input script for Band.in

Sb

```
&control
   calculation='bands'
    restart_mode='from_scratch',
    prefix='Sb'
    pseudo_dir='/home/suresh/espresso/pseudo'
    outdir='./'
!    disk_io= 'high'
!    tstress=.TRUE.
!    tprnfor=.TRUE.
/
&SYSTEM
    ibrav          = 4
    celldm(1)      = 8.2870 ! au
 !   c              = 21.6358 ! au
    celldm(3)      = 2.6108
    ecutwfc        = 80
```

```
   ecutrho       = 800
   nat           = 6
   ntyp          = 1
   nbnd          = 20
   occupations   = 'smearing'
   smearing      = 'mv'
   degauss       =  0.001
/
&ELECTRONS
   conv_thr        =  1.0d-07
   electron_maxstep = 200
   mixing_beta     = 0.7
   startingpot     = 'atomic'
   startingwfc     = 'atomic+random'
/
ATOMIC_SPECIES
  Sb 121.76  Sb.pbe-n-kjpaw_psl.1.0.0.UPF
ATOMIC_POSITIONS {crystal}
  Sb  0.000000000        0.000000000        0.266833984
  Sb  0.000000000        0.000000000        0.733165974
```

```
 Sb  0.666666667        0.333333335        0.600167317

 Sb  0.666666667        0.333333335        0.066499354

 Sb  0.333333325        0.666666669        0.933500609

 Sb  0.333333325        0.666666669        0.399832683

K_POINTS {crystal_b}

5

0.00000 0.00000 0.00000 17 ! Gamma

0.50000 -0.50000 -0.50006 10 ! M

0.50000 -0.50000 0.00000 12 ! X

0.66667 -0.33333 0.50000 20 ! R

0.00000 0.00000 0.00000 17 ! Gamma
```

Bi

```
&control

   calculation='bands'

   restart_mode='from_scratch',

   prefix='Bi'

   pseudo_dir='/home/suresh/espresso/pseudo'

   outdir='./'

!    disk_io= 'high'

!    tstress=.TRUE.
```

```
!    tprnfor=.TRUE.
/
&system
    ibrav = 0
    nat = 2,
    ntyp = 1,
    nbnd = 20,
    occupations = 'smearing',
    smearing = 'mv',
    degauss = 0.01,
    ecutwfc = 65.0
    ecutrho = 260.0
/
&electrons
    mixing_beta=0.7
    conv_thr =  1.0d-08
/
CELL_PARAMETERS {angstrom}
  4.7459001541        0.0000000000        0.0000000000
  2.5683164347        3.9909045296        0.0000000000
```

```
 2.5683164347        1.4013675379        3.7367750786
ATOMIC_SPECIES
 Bi  208.98038  Bi.pbe-dn-kjpaw_psl.1.0.0.UPF
ATOMIC_POSITIONS {crystal}
 Bi   0.237000021        0.237000010        0.237000003
 Bi   0.763000115        0.762999983        0.763000050
K_POINTS {crystal_b}
 5
 0.00000 0.00000 0.00000 15 ! Gamma
 0.00000 -0.50000 -0.50000 33 ! X
 -0.24012 -0.75989 -0.50000 28 ! M
 0.00000 -0.50000 -0.00000 10 ! R
 0.00000 0.00000 0.00000 15 ! Gamma
```

List 4: Input script for Band.in

Sb

```
&bands
 prefix='Sb'
 outdir='./'
 filband='Sb.band.dat'
/
```

Bi

```
&bands
  prefix='Bi'
  outdir='./'
  filband='Bi.band.dat'
/
```

List 5: Input script for DOS.in

Sb

```
&DOS
  prefix='Sb'
  outdir = './'
  fildos = 'dos.dat'
  DeltaE = 0.001
  ngauss = -1
  degauss = 0.0025
/
```

Bi

```
&DOS
  prefix='Bi'
  outdir = './'
```

```
  fildos = 'dos.dat'
  DeltaE = 0.01
  ngauss = -1
  degauss = 0.0025
/
```

List 6: Input script for PDOS.in

Sb

```
&projwfc
  prefix='Sb'
  outdir = './'
  filpdos='Sb.pdos'
  filproj='Sb.proj'
  DeltaE = 0.01
  ngauss = -1
  degauss = 0.0025
  Emin=-10
  Emax=10
/
```

Bi

```
&projwfc
```

```
 prefix='Bi'
 outdir = './'
 filpdos='Bi.pdos'
 filproj='Bi.proj'
 DeltaE = 0.01
 ngauss = -1
 degauss = 0.0025
 Emin=-20
 Emax=20
/
```

List 7: Input script for bands plot

Sb

```
#set terminal postscript enhanced color "Helvetica" 20
#set output "Sb.band.dat.gnu"
set autoscale
unset log
set xzeroaxis lw 2 lc -1
unset xtics
set ytics -20,1
set bmargin 3
```

```
set xlabel "kpaths" offset 0,-1,0

set ylabel "E-Ef (eV)"

set label "{/Symbol G}" at 0.00,-15.4

set label "{/Symbol G}" at 1.87409,-15.4

set label "M" at 0.608534,-15.4

set label "X" at 0.802489,-15.4

set label "R" at 1.46032,-15.4

set arrow from 0.608534, graph 0 to 0.608534, graph 1 nohead

set arrow from 0.802489, graph 0 to 0.802489, graph 1 nohead

set arrow from 1.46032, graph 0 to 1.46032, graph 1 nohead

#set key 0.01,100

set xr [0.0:1.87409]

set yr [-15:5]

ef=6.1752

plot "Sb.band.dat.gnu" using 1:($2-ef) title 'bands of Sb' w l lt 2 lc rgb "black"

pause -1 "Hit any key to continue\n"
```

Bi

```
#set terminal postscript enhanced color "Helvetica" 20

#set output "Bi.band.dat.gnu"

set autoscale
```

```
 unset log
 set xzeroaxis lw 2 lc -1
unset xtics
set ytics -20,1
set bmargin 3
set xlabel "kpaths" offset 0,-1,0
set ylabel "E-Ef (eV)"
set label "{/Symbol G}" at -0.02,-20.4
set label "{/Symbol G}" at 2.22079,-20.4
set label "X" at 0.724737,-20.4
set label "M" at 1.09190,-20.4
set label "R" at 1.59333,-20.4
set arrow from 0.724737, graph 0 to 0.724737, graph 1 nohead
set arrow from 1.09190, graph 0 to 1.09190, graph 1 nohead
 set arrow from 1.59333, graph 0 to 1.59333, graph 1 nohead
 #set key 0.01,100
 set xr [0.0:2.22079]
 set yr [-20:15]
 ef=9.6470
  plot "Bi.band.dat.gnu" using 1:($2-ef) title 'bands of Bi' w l lt 2 lc rgb "black"
```

```
pause -1 "Hit any key to continue\n"
```

List 8: Input script for dos plot

Sb

```
 # plot script
set term postscript enhanced color 'Helvetica-Bold,16'
set output 'dos.ps'
set xl 'Energy (E - E_F) (eV)'
set yl 'DOS (arb unit)
set xr [-1:1]
set yr [0:5]
set ytics
Ef=6.1512
plot 'dos.dat' u ($1-Ef):($2) w l noti
set output
! ps2pdf dos.ps
! rm dos.ps
# how to execute this script? issue the followinf line on the terminal
# gnuplot plot.gp
```

Bi

```
 # plot script,

  set term postscript enhanced color 'Helvetica-Bold,16'

set output 'dos.ps'

set xl 'Energy (E - E_F) (eV)'

 set yl 'DOS (arb unit)

 set xr [-1:2]

 set yr [0:2]

set ytics

Ef=9.6485

plot 'dos.dat' u ($1-Ef):($2) w l noti

 set output

! ps2pdf dos.ps

! rm dos.ps

 # how to execute this script? issue the followinf line on the terminal

 # gnuplot plot.gp
```

List 9: Input script for plot pdos

Sb

```
 set autoscale                        #scale axes automatically
 unset log                            #remove any log-scaling
 unset label                          #remove any previous labels
 set xtics auto                       #set xtics automatically
 set ytics auto                       #set ytics automatically
set xr [4.5:7.5]
set yr [0:8.0]
set title"Partial Density of States (PDOS) of Antimony Crystal"
set xlabel "Energy(eV)"
set ylabel "PDOS"
set ytics
 set arrow 7 from 6.1612,0 to 6.1612,6 nohead ls 2 dt 1  #fermi energy
plot "atom_Sb_s.dat"using 1:2 title'Sb s orbital' with linespoints,\
"atom_Sb_p.dat"using 1:2 title'Sb p orbital' with linespoints,\
"atom_Sb_tot.dat"using 1:2 title'Sb total'with linespoints,
pause-1 "Hit any key to continue\n"  #so that the code doesnot exit automatically
set output
pause-1 "hit any key to continue\n"
```

Bi

```
set autoscale                #scale axes automatically
unset log                    #remove any log-scaling
unset label                  #remove any previous labels
set xtics auto               #set xtics automatically
 set ytics auto              #set ytics automatically
 set xr [8:10]
set yr [0:4.0]
 set title"Partial Density of States (PDOS) of Bismuth Crystal"
set xlabel "Energy(eV)"
 set ylabel "PDOS"
set arrow 10 from 9.6485,0 to 9.6485,4 nohead ls 3 dt 1  #fermi energy
plot "atom_Bi_s.dat"using 1:2 title'Bi s orbital' with linespoints,\
"atom_Bi_p.dat"using 1:2 title'Bi p orbital' with linespoints,\
"atom_Bi_d.dat"using 1:2 title'Bi d orbital' with linespoints,\
"atom_Bi_tot.dat"using 1:2 title'Bi total'with linespoints,
 pause-1 "Hit any key to continue\n"  #so that the code doesnot exit automatically
 set output
 pause-1"hit any key to continue\n"
```